Dynamic of organic matter and meiofaunal community on a river-dominated shelf (Rhône prodelta, NW Mediterranean Sea): Responses to river regime

Pruski Audrey M. [1, *], Rzeznik-Orignac Jadwiga [1], Kerhervé Philippe [2], Vétion Gilles,
Bourgeois Solveig [1], Peru Erwan [1], Brosset Pablo [1], Toussaint Flora [3], Rabouille Christophe [3]

[1] Sorbonne Université, CNRS, Laboratoire d'Ecogéochimie des Environnements Benthiques, LECOB, F-66650, Banyuls-sur-Mer, France
[2] Université de Perpignan Via Domitia, CNRS, Centre de Formation et de Recherche sur les Environnements Méditerranéens, CEFREM, F-66860, Perpignan, France
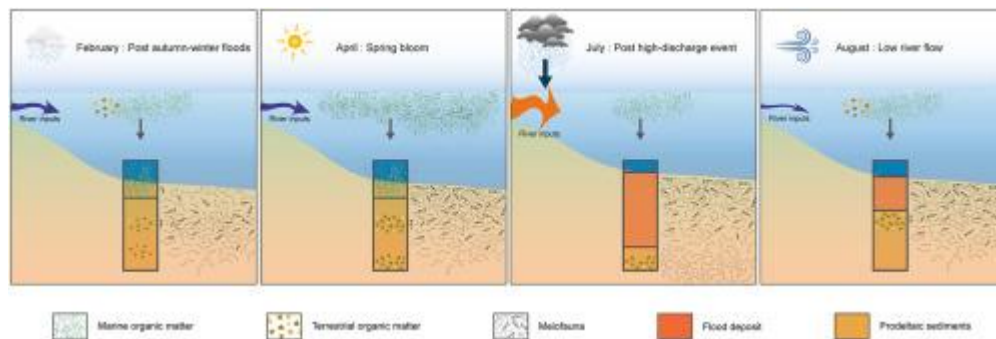[3] Laboratoire des Sciences du Climat et de l'Environnement, LSCE/IPSL,CEA-CNRS-UVSQ-Université Paris Saclay, 91198, Gif-sur-Yvette, France

* Corresponding author : Audrey M. Pruski, email address : audrey.pruski@obs-banyuls.fr

Abstract :

In the oligotrophic context of the Mediterranean Sea, riverine inputs of particulate organic matter represent an important source of food for benthic communities. However, since most of these inputs are delivered during short, but intense flood events, communities living in the vicinity of river mouths are also exposed to strong and frequent physical disturbances. A very tight and complex relationship links river dynamic and macrofaunal communities in Mediterranean deltas, but less is known on the response of meiobenthic communities to river regime. In 2010, sediments cores were collected in the Rhône River prodelta in winter and spring before the flooding of the Rhône River tributaries in June, and then twice in the early and late summer. The hypothesis was that increased runoff and export of terrigenous material would induce major changes in the sediment biochemistry, which would in turn trigger modifications in abundances and vertical distribution of the meiofauna. The origin and quality (lability, degradation state) of the different pools of organic matter preserved in these recent sediments were determined using bulk geochemical and molecular analyses (fatty acids, amino acids). Vertical profiles of descriptors for organic matter origin and quality revealed major changes in the nature of the inputs occurring at monthly time scales. Inputs of plant detritus from autumnal and winter flood events were still visible in the cores collected in February and April. A few days after the June 2010 high-discharge event, a newly deposit (∼7 cm) containing soil organic matter has recovered the prodeltaic sediments and the resident meiofaunal community, but at the end of August only 2 cm of this deposit remained. Multivariate analyses furthermore highlighted that the meiofaunal community was driven by both the trophic conditions and deposition of a new sediment layer driven by the hydrological regime of the Rhône River. In April, increased abundances of meiofauna were observed in response to the sedimentation of labile organic matter after the spring bloom. The June high-discharge event affected the meiofauna with a reduction of its abundance and the burial of the resident meiobenthic community. However, the meiofauna recovered in less than two months after this disturbance, showing the strong resilience of this component of the benthic ecosystem in this high energy environment.

Graphical abstract

| February : Post autumn-winter floods | April : Spring bloom | July : Post high-discharge event | August : Low river flow |

Marine organic matter · Terrestrial organic matter · Meiofauna · Flood deposit · Prodeltaic sediments

Highlights

► Vertical distribution of sedimentary organics varies at a monthly time scale. ► Origin determines organic matter quality. ► Meiofaunal abundances are driven by trophic conditions and river regime. ► Rapid response of meiofauna to the sedimentation of phytodetritus. ► High resilience of meiofauna to flood disturbance.

Keywords : Mediterranean Sea, Rhône River, high-discharge event, physical disturbance, marine sediments, organic matter, meiofauna

49   1. Introduction

50   Rivers represent the main source of fresh water, nutrients, sediments and terrestrial organic

51   carbon (OC) to the coastal ocean. Continental shelves influenced by large to medium-sized rivers

52   consequently account for some of the most biologically productive marine systems on Earth and have

53   great ecological, biogeochemical, social and economic values (Day et al., 2019b). River flow dynamic,

54   land use, coastal circulation, resuspension and meteorological events are all parameters that exert

55   some level of control on the delivery and dispersal of riverine inputs of sediments and OC on the shelf.

56   Human activities such as deforestation, agriculture, urbanisation, fluvial regulation and diversion affect

57   the land-ocean export, both quantitatively and qualitatively (Bianchi and Allison, 2009). These

58   transitional areas are also particularly vulnerable to climate-driven disturbances associated with global

59   warming, sea-level rise and the increasing frequency and intensity of storms (O'Leary et al., 2017).

60   How natural and anthropogenic changes in the delivery of terrestrial OC to continental shelves will

61   affect global OC budgets remains largely uncertain (Bauer et al., 2013). Likewise, benthic communities

62   play a central role in the cycling and burial of OC in estuarine ecosystems, but they are particularly

63   exposed to combined anthropogenic stressors (Akoumianaki et al., 2013, 2006; Martin et al., 2019).

64   Given this, the question is how and to what extent, changes in river inputs have an impact on benthic

65   communities and the regulating services they provide.

66   Deltas are peculiar estuaries that form where sand and mud supply exceeds sediment

67   dispersal. Their existence and functioning are therefore closely linked to river inputs (Giosan et al.,

68   2014). A plethora of river delta systems have formed in the microtidal wave-influenced setting of the

69   Mediterranean Sea (Besset et al., 2017). The watersheds and fluvial regime of most Mediterranean

70   deltas, including the Ebro, Rhône, Po and Nile, have undergone severe modifications to accommodate

71   human activities (Day et al., 2019a). Despite considerable efforts to control the runoff of these rivers,

72   the export of particulate matter takes place primarily during high discharge flood events triggered by

73   intense rainfalls or oceanic storms (Antonelli et al., 2008). Depending on the season and drainage

74   basin affected, the magnitude and nature of the particulate organic matter (POM) exported during

75   these events are highly variable with inputs of fossil OC, eroded soils, riparian vegetation or

76   phytoplankton (Antonelli et al., 2008; Cathalot et al., 2013; Harmelin-Vivien et al., 2010; Higueras et

77   al., 2014; Marion et al., 2010; Tesi et al., 2008). Meteorological and hydrological drivers are thus

78   expected to control the supply and quality of the POM delivered to the shelf as well as its

79   bioavailability for the benthic fauna. Moreover, extreme flooding events results in the rapid deposition

80   of fine terrigenous particles which have significant effects on the structure and function of

81   macrobenthic communities (Cardoso et al., 2008; Lohrer et al., 2004; Norkko et al., 2002). For

82   instance, off the Rhône River, the proliferation of opportunist species taking advantage of flood

83   deposits has been observed in the months following major events (Salen-Picard et al., 2003). A very

84   tight and complex relationship links river dynamic and macrofaunal communities in Mediterranean

85   deltas (Akoumianaki and Nicolaidou, 2007; Bonifácio et al., 2014; Hermand et al., 2008; Salen-Picard

86   et al., 2003). By contrast, meiobenthic communities (animals retained between 40 μm and 1 mm

87   mesh size of sieves; Giere, 2009) from deltaic systems have received little attention (Danovaro et al.,

88   2000; Guidi-Guilvard and Buscail, 1995; Palacín et al., 1992, Semprucci et al., 2019) at the notable

89   exception of foraminiferans (Fontanier et al., 2008; Franzo et al., 2019; Goineau et al., 2012). The

90   meiofauna has an important role in the functioning of benthic ecosystem, contributes significantly to

91   the diet of many other animals (Coull, 1990), and facilitates mineralisation of organic material (Coull,

92   1999; Gee, 1989; Riera and Hubas, 2003). Because of their small size, lack of larval stage and shorter

93   generation time, meiobenthic organisms respond more successfully than the macrofauna to changes

94   in environmental conditions (Balsamo et al., 2012). As such, meiofaunal communities have been

95   widely used to monitor the effects of both natural and anthropogenic perturbations in aquatic

96   ecosystems (Coull and Chandler, 1992; Gambi et al., 2003; Schratzberger and Ingels, 2018, Semprucci

97   et al., 2018). Although the meiofauna appears as a good bioindicator of organic enrichment and

98   physical disturbance in coastal areas (Gambi et al., 2003), there is a paucity of studies focusing on their

99   response to river inputs (Danovaro et al., 2000; Guidi-Guilvard and Buscail, 1995; Palacín et al., 1992;

100   Pelletier et al., 1999).

101   In this study, the response of meiofaunal communities to the dynamic of river inputs is

102   discussed. In 2010, we had the opportunity to study the impact of a high-discharge event of the Rhône

103   River, the largest Mediterranean river. Sediments were collected in the winter and spring before this

104   period and afterwards, twice in the early and late summer. The hypothesis was that this extreme

105   event would induce major changes in the sediment biochemistry, which would in turn trigger

106   modifications in abundances and vertical distribution of the meiofauna. The specific aims of the

107   present study were (1) to evaluate how the Rhône River regime affect sediment biochemistry in the

108   prodelta at a seasonal time scale, (2) to investigate whether the main taxa of the meiofauna respond

109   to changes in river inputs, and (3) to determine which of the investigated environmental parameters

110   (i.e. grain-size, porosity, sedimentary organic matter composition, stable isotopic values…) were the

111   most pertinent to illustrate the observed trends. A particular attention was paid at determining the

112   origins and quality of the POM delivered by the Rhône River, as it represents fresh sources of detritus

113   for benthic organisms.

114

115   2. Materials and methods

116   2.1. Regional setting and study area

117   The Rhône River, now the main river in the Mediterranean Sea since the damming of the Nile,

118   links the Rhône glacier in the Swiss upper Alps to the Camargue delta on the French coast of the

119   Mediterranean Sea (the Gulf of Lion). It is mainly an Alpine river, which drains a relatively small

120   (95,000 km^2), but highly diversified, watershed exhibiting a strong geological heterogeneity (Olivier et

121   al., 2009). The Rhône catchment includes several climatic zones (mountainous, oceanic and

122   Mediterranean) resulting in a very complex hydrological regime and a strong inter annual variability

123   (Pont et al., 2002). Typical of Mediterranean rivers, the runoff of the Rhône is characterised by

124   flooding events triggered by intense rainfalls in autumn and snowmelt in spring. As a consequence,

125   solid export to the Gulf of Lion occurs mainly during short, but intense high-discharge events

126   (Antonelli et al., 2008). Riverine particulate inputs undergo a rapid deposition near the river mouth in

127 the prograding prodelta (Maillet et al., 2006). The unconsolidated sediments are frequently

128 resuspended by episodes of strong winds or by near bottom currents (Ulses et al., 2008). The study

129 area is located at 2.5 km of the Rhône River mouth in the prodelta area (Fig. 1).
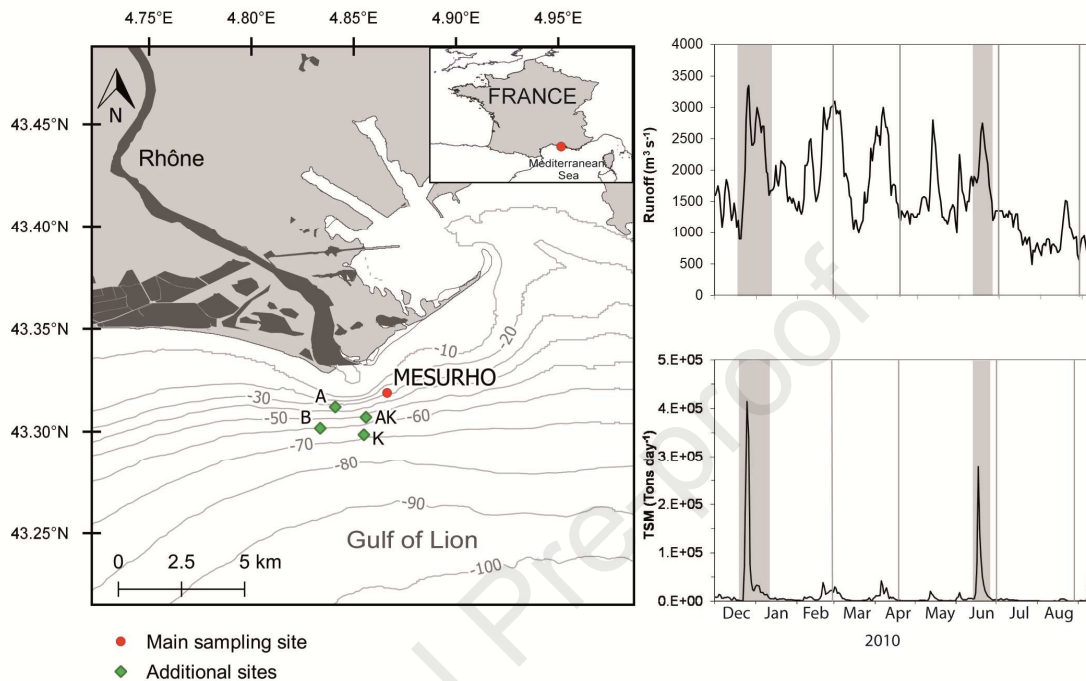
130

131 **Figure 1: Location of the sampling sites in the Gulf of Lion (left) and Rhône River runoff and total**
132 **suspended matter (TSM) concentration for 2010 (right).** Rhône data were measured at the SORA
133 Observatory Station in Arles, the most downstream gauge station, 40 km upstream the mouth. The
134 vertical bars indicate the sampling dates and the grey areas represent periods of high solid discharge
135 rate.

136

137 2.2. Hydrological and climatic conditions

138 Mean daily discharge data from the Arles gauging station were provided by the CNR
139 (Compagnie Nationale du Rhône, the main hydropower company on the Rhône River). Daily total
140 suspended matter (TSM) concentrations measured in water samples collected at the Rhône
141 observatory station at Arles (SORA) were provided by the MOOSE network (Mediterranean Oceanic
142 Observing System for the Environment – http://www.moose-network.fr). Monthly weather reports
143 were provided by Météo France.

144

145

146   2.3. Sediment sampling

147   The sampling targeted four contrasted periods in 2010: winter (20th February), spring (18th

148   April), early (1st July) and late summer (28th August). Sediment cores were collected at station

149   MESURHO (43°19.2 N, 4°52 E, 20 m depth) from the board of the Téthys II R/V using a multicorer MUC

150   8/100 (Oktopus GmbH) during the field campaigns MESURHOBENT 1, 2, 3 and 4 (Rabouille, 2010a, b,

151   c, d). At each sampling date, four undisturbed sediment cores (9.5 cm of diameter and 60 cm of

152   height) were processed on board and sliced into seven horizontal layers (0–0.5, 0.5–1, 1–2, 2–3, 3–5,

153   5–7 and 7–10 cm). Since previous studies in the prodelta area have shown that variability among cores

154   was low (Bourgeois et al., 2011; Cathalot et al., 2010; Pastor et al., 2011a), one core was conditioned

155   in this study for sediment characterisation. Sediment layers were carefully homogenised, distributed

156   in two aliquots and immediately frozen at -20°C. Sediment layers from the three other cores were

157   preserved in 70% alcohol for meiofaunal analysis. Visual observation of the sediment cores used in this

158   study showed no signs of burrows, biogenic structures, oxic voids or large macrofauna, suggesting low

159   bioturbation activity.

160

161   2.4. Assessment of sediment characteristics

162   Sediment granulometry was assessed using a Malvern® Mastersizer 2000 laser diffraction

163   particle size analyser. Porosity (φ) was calculated by determining water mass loss during drying

164   assuming a value of 2.63 g.cm^{-3} for grain size density and 1.03 g.cm^{-3} for pore water density. Sediment

165   granulometry, and porosity were determined in triplicate for each sample.

166   Elemental and biochemical analyses were performed on freeze-dried sediments. The analytic

167   protocols for total organic carbon (TOC), bulk stable carbon isotopes (δ^{13}C), total hydrolysable amino

168   acids (THAA) and fatty acids have been described in Fagervold et al. (2014).

169   Enzymatically hydrolysable amino acids (EHAA), which correspond to the fraction of amino

170   acids assumed to be bioavailable for benthic deposit-feeders, were extracted by the biomimetic

171 approach of Mayer et al. (1995). THAAs and EHAAs were analysed by reverse phase high-performance

172 liquid chromatography (HPLC, Gynkotek-Dionex system) following precolumn derivatisation with

173 orthophtaldialdehyde (Lindroth and Mopper, 1979). The isoindol derivatives were separated on a C18-

174 HPLC column using a non-linear gradient of methanol-acetate buffer and were detected by

175 fluorescence at 450 nm using an excitation wavelength of 335 nm (Bourgeois et al., 2011).

176   Fatty acid, THAA and EHAA concentrations were normalised to total organic carbon.

177

178 2.5. Assessment of meiofaunal abundance and taxonomic composition

179   The sediment samples were sieved through 1000 and 40 µm mesh simultaneously. The

180 fraction retained on the 40 µm sieve was collected and centrifuged with Ludox HS 40 (density 1.15) as

181 described by Heip et al. (1985). The organisms in the supernatant were collected and rinsed on a 40

182 µm mesh to remove Ludox and preserved in 70% alcohol. All meiobenthic organisms were counted

183 and classified to higher taxon under a stereomicroscope, after staining with rose Bengal. A sample

184 splitter, Motoda-box (Motoda, 1959) was used to obtain an aliquot containing about 1000 organisms,

185 for the abundance estimations of nematodes and copepods. The number of other meiobenthic taxa

186 was too low to evaluate on split samples, they were thus counted on the whole sample. Total density

187 of meiofauna and of the main representative taxa (nematodes, copepods, annelids, cumaceans,

188 turbellarians, foraminiferans, and kinorhynchs) were determined (number of individuals/10 cm^2) for

189 the four sampling dates. Mean density based on the 3 cores were calculated for each layer. Note that

190 the Ludox extraction is less efficient for organisms with shells, like foraminiferans, molluscs or

191 ostracods, and that the abundances were thus underestimated for these taxa.

192

193 2.6. In situ microprofiling of dissolved oxygen and DOU calculation

194   A benthic lander carrying a benthic microprofiler (Unisense®) was deployed to measure *in situ*

195 microprofiles of dissolved oxygen (Cai and Reimers, 1993; Rabouille et al., 2003; Rassmann et al., 2020

196 and references therein). The benthic lander was deployed in April, July and August 2010 at a maximum

197 of 5 stations, except in August because of bad weather conditions. These stations encompass the

198 MESURHO station, another proximal station located in the South of the Rhône River (A), and 3 other

199 stations located in the Rhône prodelta (AK, B and K, Fig. 1).

200 Four oxygen microelectrodes were simultaneously deployed, and vertical depth profiles were

201 measured with a 200 μm resolution together with a resistivity electrode. As their response to

202 variations in oxygen concentrations is linear (Boudreau and Jorgensen, 2001), the O_2 microelectrodes

203 were calibrated with a two-point calibration technique using the bottom water O_2 concentration

204 determined by Winkler titration and the anoxic pore waters. Signal drift of O_2 microelectrodes during

205 profiling was checked to be less than 5 %. Diffusive oxygen uptake (DOU) rates were calculated using

206 Fick's first law (Berner, 1980, Eq. 3),

207 $$DOU = -\emptyset \cdot D_s \cdot \frac{d[O_2]}{dz}\Big|_{z=0} \qquad (3)$$

208 where ϕ is sediment porosity, Ds the diffusion coefficient in the sediments ($cm^2\ s^{-1}$), and

209 $\frac{d[O_2]}{dz}\Big|_{z=0}$ is the oxygen gradient below the sediment water interface ($\mu mol\ cm^{-4}$). For the calculations,

210 the gradient between 0 and 400 μm in the sediment was consistently used. The Ds coefficients were

211 adjusted for diffusion in a porous environment according to: $D_s = \frac{D_0}{(1+3\cdot(1-\emptyset))}$ with the diffusion

212 coefficient in free water (D_0) taken from Broecker and Peng (1974) and recalculated at *in situ*

213 temperature using Li and Gregory (1974).

214

215 2.7. Data analysis

216 The amount, sources, and quality of the sedimentary organic matter (OM) in the Rhône

217 prodelta were assessed with a suite of bulk and molecular descriptors. The list of the parameters used

218 in this study is provided in Table 1 with their interpretation. The degradation index (DI) was calculated

219 from the molar composition of the THAA hydrolysates (Dauwe et al., 1999a). This index synthesises

220 subtle changes in the amino acid composition linked with diagenesis into a univariate variable

221 indicative of OM degradation stage, whose value decreases with increasing degradation. We applied

222 the same calculation on the EHAA composition of the flood deposit. In this case, the index (DI_{EHAA})

223 provided information on the degradation stage of the pool of amino acids that may be assimilated by

224 benthic organisms. The reactivity index [RI=(tyrosine+phenylalanine)/(β-alanine+ɣbutyric acid)] is

225 another indicator of OM degradation (Jennerjahn and Ittekkot, 1997). It takes into account two

226 opposite trends: the reactive aromatic amino acids, tyrosine and phenylalanine, are rapidly degraded

227 in decaying OM, whereas their decarboxylation products, β-alanine and ɣ-butyric acid, consistently

228 increase with microbial degradation (Alkhatib et al., 2012; Jennerjahn and Ittekkot, 1997).

229 A one-way ANOVA was used to analyse variations in total meiofaunal abundance whereas

230 two-ways ANOVA were performed to test for differences in meiofaunal vertical distribution with time,

231 with sediment depth and time x sediment depth. Abundances were double square root transformed in

232 order to meet the assumptions for ANOVA (homogeneity of variances, normally distributed residuals).

233 A Tukey Honest Significance Test (HSD) test was applied when significant differences were detected

234 between means. Analyses of variance were run with XLSTAT (V4.01).

235 A principal component analysis (PCA) was then performed to reveal trends in OM composition

236 that could help us retrace the recent history of riverine particle inputs in the prodelta. Prior to PCA, a

237 correlation analysis of the environmental variables was performed to identify variables that were

238 highly correlated, retaining only one of these variables. PCA was combined to hierarchical clustering of

239 the PCA components (HCPC), which determines clusters of samples that present homogenous

240 characteristics (Husson et al., 2010). The HCPC was performed on the 5 first components of the PCA

241 (accounting for 91% of the total variance) using Ward's agglomerative method and a Euclidean

242 distance. PCA and HCPC were performed using R software (3.4.4) with the package 'Rcmdr –

243 Factominer' (Lê et al., 2008).

244 Relationships between the abundance of meiofaunal taxa and factors, representing sediment

245 characteristics, were summarised using a Canonical Correspondence Analysis (CCA) (ter Braak, 1986)

246 performed with the R package 'vegan' (Oksanen et al., 2016). CCA allowed to simultaneously visualise

247 the abundances of the principal meiofaunal taxa, the optimal niches (sample corresponding to

248   sediment depth × date) with the environmental parameters (Borcard et al., 2011). The environmental

249   variables identified by PCA were first retained. The "vif.cca" function of 'vegan' was then used to

250   identify redundant constraints (i.e. environmental variables with variance inflation factors >10) and

251   were removed from the analysis to reduce collinearity. CCA was finally performed on square root

252   transformed abundances to reduce the weight of abundant taxa and a subset of standardised

253   environmental variables describing the quality of food available for the meiofauna (δ^{13}C, C/N ratio,

254   normalised concentration in EHAA, EHAA/THAA ratio, DI, % Algal PUFA) or related to sediment

255   properties (porosity, % clay, and $CaCO_3$). The statistical significance of the overall relationship and of

256   the canonical axes were evaluated using Monte Carlo permutation tests (999 permutations). The CCA

257   ordination diagram displayed samples and taxa as points and environmental variables as vectors

258   (Borcard et al., 2011). Finally, the relative importance of the explanatory variables was evaluated by

259   forward selection followed by Monte Carlo permutation tests (999 permutations) using the "ordistep"

260   function of 'vegan' (Blanchet et al., 2008). With this method, all variables are ranked on the basis of

261   their marginal effects (i.e. considering each variable as the sole constraining variable) and conditional

262   effects (i.e. forward selection on the best descriptors and evaluation of the fit of each variable in

263   conjunction with the variable(s) already selected).

264   Result outputs for ANOVA and multivariate analyses are provided in the supplementary

265   material.

266

267   **3. Results and discussion**

268   **3.1. Hydrological and climatological conditions**

269   In 2010, the French Mediterranean coast experienced a cold and rainy winter with strong

270   winds dominated by Mistral. Rains were frequent, but moderate with Rhône water discharge reaching

271   2500m^3 s^{-1} ten days before February sampling and 3000m^3 s^{-1} on the sampling date (Fig. 1). The

272   organic content of the total suspended matter (TSM) was high (TOC= 7.81% on the 12th of February

273   2010, Kerhervé unpublished result). March was also rainy and windy. Two minor floods occurred

274   before the April sampling, but TSM only slightly increased during these events. In April, the weather

275   was fair with little wind and precipitation, but liquid discharge rates were high, possibly because of

276   snow melting. As a consequence, TSM increased above 100mg.L^{-1}. On the 15th and 16th of June 2010,

277   exceptional stormy rains (40cm per day) have generated severe flooding in south-eastern France. This

278   rare and deadly flash flood event is believed to be the most important since 1827 (Payrastre et al.,

279   2012). Rainfalls mostly affected the southeast tributaries of the Rhône River (the Durance, the Buëch,

280   the Verdon, etc.) causing their overflow. The runoff of the Rhône River peaked at 2600m^{3}.s^{-1}, while

281   solid discharge reached 2.8 10^{5} tones on June 16, 2010. In the days before return to normal runoff,

282   the Rhône brought approximately one fourth of the annual solid input for 2010. The summer was dry

283   and hot. The daily runoff rate was below the mean inter annual flow rate of 1700 m^{3}s^{-1} and was typical

284   of low river flow (500-1000 m^{3}s^{-1}). July was characterised by strong winds generally oriented N-NW (12

285   to 13 days of Mistral). The wind changed of direction on the 26th of July (S) and generated a storm

286   regime. Meteorological conditions were similar on August with episodes of strong winds.

287

288   3.2 Oxygen penetration depth and metabolic activity traced by diffusive oxygen uptake (DOU) in the

289   Rhône prodelta

290   The oxygen microprofiles recorded *in situ* at station MESURHO display a large decrease below

291   the sediment-water interface over depth of a few millimetres, below which the sediment was

292   completely anoxic (Fig. 2). A clear change in time for the oxygen penetration depth (OPD) is visible on

293   figure 2 with average values of 1.4 ± 0.5 mm in April 2010, 2.6 ± 0.5 mm in July 2010, and 2.4 ± 0.2

294   mm in August 2010.
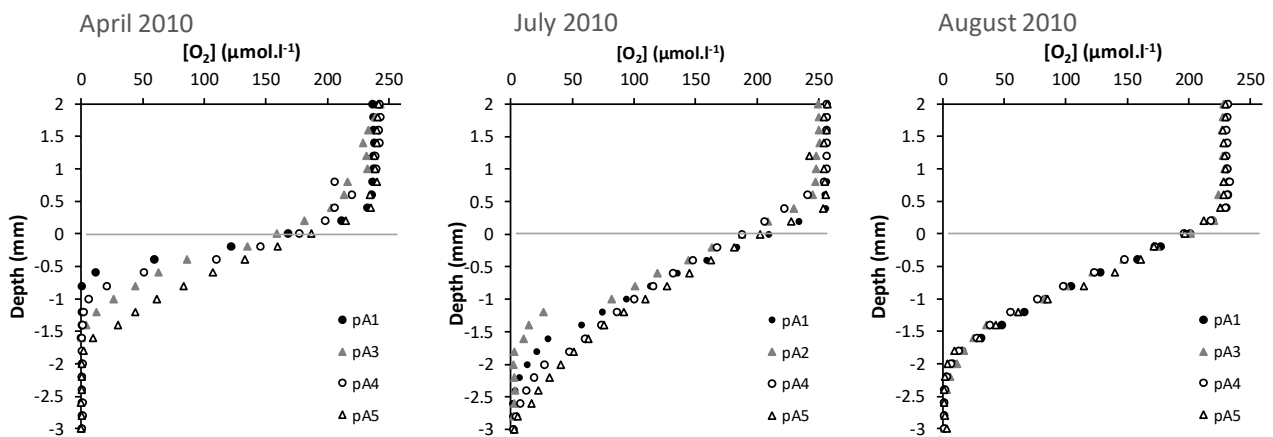
295   **Figure 2: Dissolved oxygen microprofiles at the sediment-water interface recorded *in situ* at the**

296   **MESURHO station in April, July, and August 2010.** Each symbol represents a single electrode profile.

297   The line at 0 mm indicates the sediment surface.

298

299   This increase in OPD is accompanied by a decrease of DOU (Table 2), which is a proxy of the metabolic

300   activity in the sediments based on organic matter mineralisation (Cathalot et al., 2010; Rassmann et

301   al., 2020). The DOU recorded at 5 stations in the prodelta show a decrease from April to July, with a

302   levelling in August for the only record that we have at the MESURHO station. The decrease of DOU at

303   the spring-summer transition in 2010 contrasts with the normal spring-summer situation with fresh

304   organic matter deposition and bottom water warming, which generates more mineralisation in

305   surface sediments (Lansard et al., 2008). This unusual decrease in early summer could be related to

306   the high-discharge event in June and the deposition on the seabed of low reactivity material as

307   happened in 2008 during a flood carrying significant amount of material from the Durance tributary

308   (Cathalot et al., 2010). The decrease was more pronounced for stations MESURHO and AK (~ 40%

309   decrease), which are directly under the influence of the Rhône River inputs, and more limited for

310   stations B and K, suggesting lower disturbance with increasing distance from the river mouth.

311

312

313 3.3. Short-term chronicle of particulate organic matter inputs in the Rhône prodelta

314   Short sediment cores collected in deltaic areas are useful records of the recent history of

315 riverine POM inputs in coastal areas (Cathalot et al., 2010; Leithold and Hope, 1999). The down-core

316 evolution of sedimentary OM composition provides insights on temporal changes in the characteristics

317 of the POM available for the benthic fauna (Goineau et al., 2012). Clearly, the down-core profiles of

318 organic compounds are far from a textbook situation with steady inputs of OM from the overlying

319 water and progressive degradation on the seafloor (see for instance TOC profiles, Fig. 3). Likewise,

320 descriptors of OM origin (δ^{13}C, fatty acid subgroups) and quality (C/N, EHAA/THAA, DI, RI) point to

321 major changes in the nature of the inputs occurring at a monthly time scale (Fig. 3).

322   In February, sampling occurred early at the very onset of a Rhône River flood. High organic

323 contents were observed through the sedimentary column, with an integrated TOC content of 1.4% for

324 the ten first centimetres of sediment (Fig. 3). The normalised concentrations in THAA and fatty acids

325 were also high. Descriptors of OM quality and origins revealed strong differences between the surface

326 sediment and the layers below. Phytoplankton markers were only found in the upper layer indicating

327 either the rapid degradation of this labile fraction within the sediments or a recent pulse of POM

328 deriving from microalgae. This assumption is further supported by an enriched δ^{13}C value as well as by

329 descriptors of OM quality (DI, RI, and EHAA/THAA ratio), which exhibited slightly higher values on the

330 surface than in the layers below (Fig. 3). Subsurface and deeper layers were enriched in coarse

331 material and markers of plant detritus (long chain fatty acids) and had a constant C/N ratio of ~10.

332 These biomarkers associated to high TOC contents and a coarser material are consistent with the

333 preservation of plant detritus brought in autumn and winter.
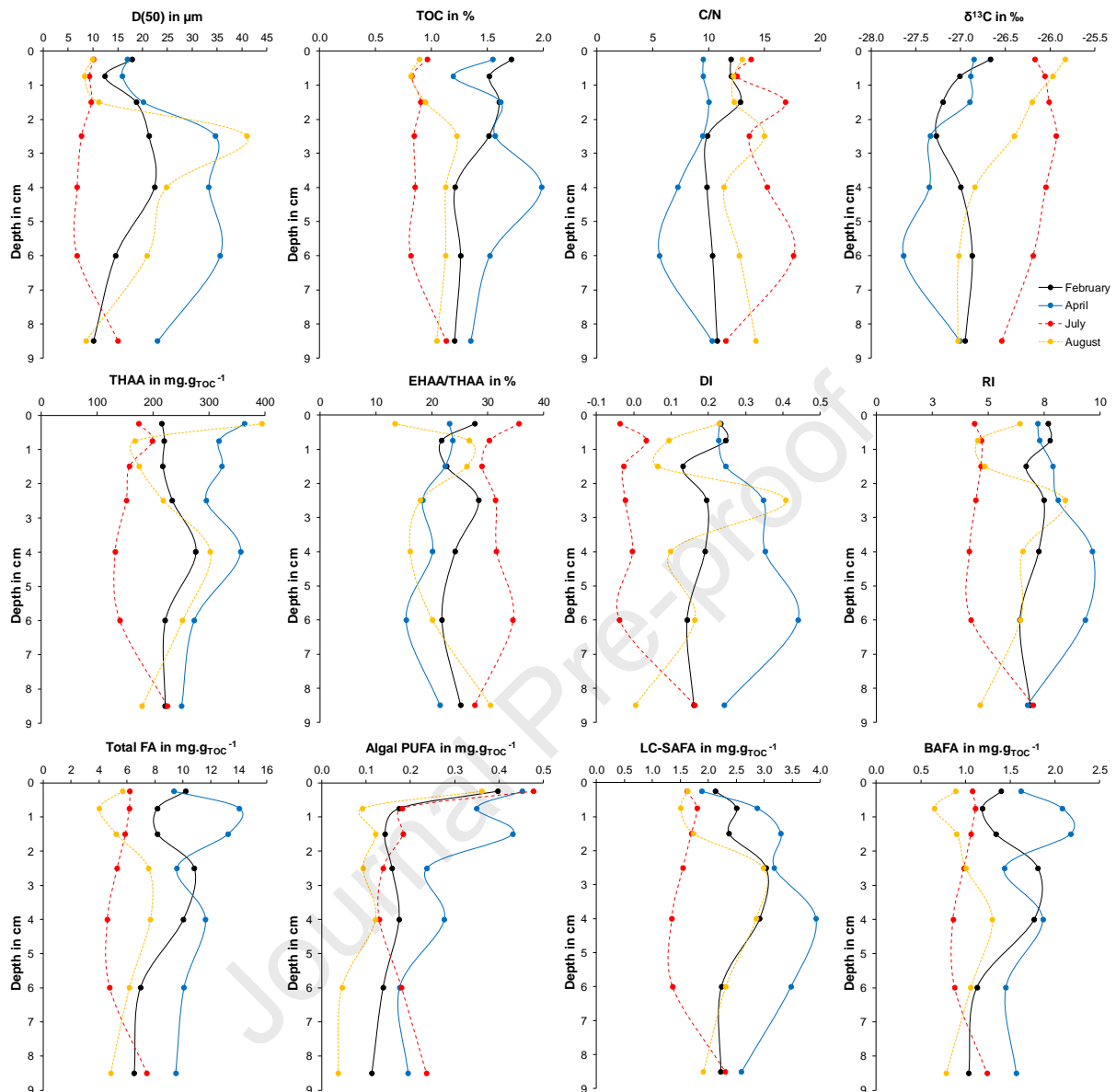
Figure 3: Down-core evolutions of sediment properties at the MESURHO station in February, April, July, and August 2010. D(50)= median grain size, TOC= total organic carbon, C/N= molecular carbon to nitrogen ratio, δ^{13}C= bulk stable isotope value, THAA= normalised total hydrolysable amino acid concentration, EHAA/THAA= proportion of enzymatically hydrolysable amino acids, DI= degradation index value, RI= reactivity index, Total FA, Algal PUFA, LC-SAFA and BAFA= TOC-normalised concentrations in total fatty acids, algal polyunsaturated fatty acids, long chain saturated fatty acids and bacterial fatty acids.

343   In April, sedimentary characteristics were more heterogeneous on the 10cm layer than during

344   the winter (Fig. 3). TOC content was still high and comparable to February in the surface sediment, but

345   at 3-7cm depth, a layer enriched in markers of plant detritus was observed. At the surface, high

346   concentrations in planktonic markers were again suggestive of phytoplankton inputs. Organic carbon,

347   amino acids and fatty acids tended to be higher in the subsurface sediments. This coarser subsurface

348   layer was also less degraded (higher DI and RI) with a lower bioavailability of the amino acid pool.

349   Globally, this suite of descriptors indicates that plant detritus have been exported during the two

350   floods that preceded the sampling, or that earlier deposits in the mud belt have been remobilised.

351   Porosity was also discontinuous, in agreement with the successive deposition of different layers of

352   material.

353   The grain size distribution shows the deposition of about 7 cm of fine particles on the

354   sediment after the torrential rainfalls in June (Fig. 3, 96% of particles <63µm). The sudden peak of TSM

355   (Fig. 1) certainly accounted for this deposit, which was depleted in organic carbon and nitrogen. The

356   flood deposit was also depleted in labile components such as fatty acids and hydrolysable amino acids

357   (on average only ~7% of the TOC was found in the THAA) and was globally more degraded (lower DI

358   and RI) than the material delivered during periods of normal discharge. The characteristics of this fine

359   material recall the one delivered by the Rhône River during the flood of the Durance tributary in June

360   2008 (Bonifácio et al., 2014; Pastor et al., 2018). Following this event, a flood deposit of ~30 cm was

361   observed in the prodelta area (Cathalot et al., 2010). This organic-poor material had a peculiar δ^{13}C

362   signature (-25.8‰) and displayed a Δ^{14}C of -495‰ in relation with the refractory nature of the eroded

363   watershed and the flushing of the Serre-Ponçon dam on the Durance (Cathalot et al., 2013; Copard et

364   al., 2018). The decrease in remineralisation activity in the surface sediments after these two events is

365   a further indication that the deposited material was poorly reactive (Table 2).

366   The trend for lower porosities at the end of August suggests that the summer conditions

367   allowed the muddy deposits to settle and become more compact (Table S1, supplementary material).

368   This is consistent with the concomitant stratification of the microbial community described by

369   Fagervold et al. (2014) at this station. Organic content was still low, but OM characteristics indicate

370   intense reworking of the sediments since July (Fig. 3). $\delta^{13}C$ values ranged from "flood signature" of the

371   tributaries (~ -26‰) in surface to the usual winter value of the Rhône (~ -27‰). Below the first two

372   centimetres, which kept the flood imprint, the sediment was enriched in TOC, amino acids, fatty acids,

373   and long chain fatty acids. The down-core evolution of the DI is difficult to interpret. In the surface

374   layer (0-0.5cm), the DI value was similar to values found in February and April on the top of the cores

375   and may be indicative of the recent export of TSM by the Rhône River. Values for the 0.5-1 and 1-2cm

376   layers were closed to those found in the flood deposit, between 2-3cm depth DI was similar to values

377   measured in the April layer enriched with macrodetritus, and below DI was lower indicative of a more

378   degraded pool of POM. Grain size followed the same trend as DI in good consistency with the

379   hypothesis that the 2-3cm layer corresponded to sediments enriched in coarse macrodetritus. The

380   proportion of bioavailable amino acids (EHAA/THAA) was also extremely variable along the sediment

381   depth consistent with inputs of different sources of POM and non-steady state conditions.

382   Taken together all these results show that the flood deposit formed a thinner layer at the end

383   of the summer in comparison to what settled in June. Estimation of the thickness of this layer is about

384   1.5 to 2 cm depending on the parameters used. Compaction cannot entirely account for the reduction

385   of the thickness of the flood deposit. Erosion is the most likely explanation. Strong winds occurred in

386   July (26th) causing the resuspension of sediments at the MESURHO buoy (Lorthiois, 2012). The author

387   described the sediment dynamic during this event as the resuspension of the non-consolidated

388   sediments and their near bottom transport offshore. Dufois et al. (2014) have demonstrated that

389   bottom erosion could be an important process for the sediment dynamic in the prodelta area during

390   moderate river discharge and energetic events. Above the remaining flood deposit, some inputs of

391   fresh suspended particulate matter (DI= 0.23) enriched in labile biogenic compounds (amino acids and

392   fatty acids) have settled during the summer (Fig. 3). Underneath the flood deposit, older consolidated

393   deposits from the autumn, winter and/or spring were found.

394

395

396

397 **3.4. Sources and lability of the sedimentary organic matter in the Rhône prodelta**

398   Down-core evolutions of bulk and molecular descriptors of sedimentary organics in the

399 prodelta highlight the occurrence of several pools of OM, whose dynamic of delivery is related to

400 season and river regime. A PCA was performed to define the biochemical properties of these different

401 pools of OM (Fig. 4).
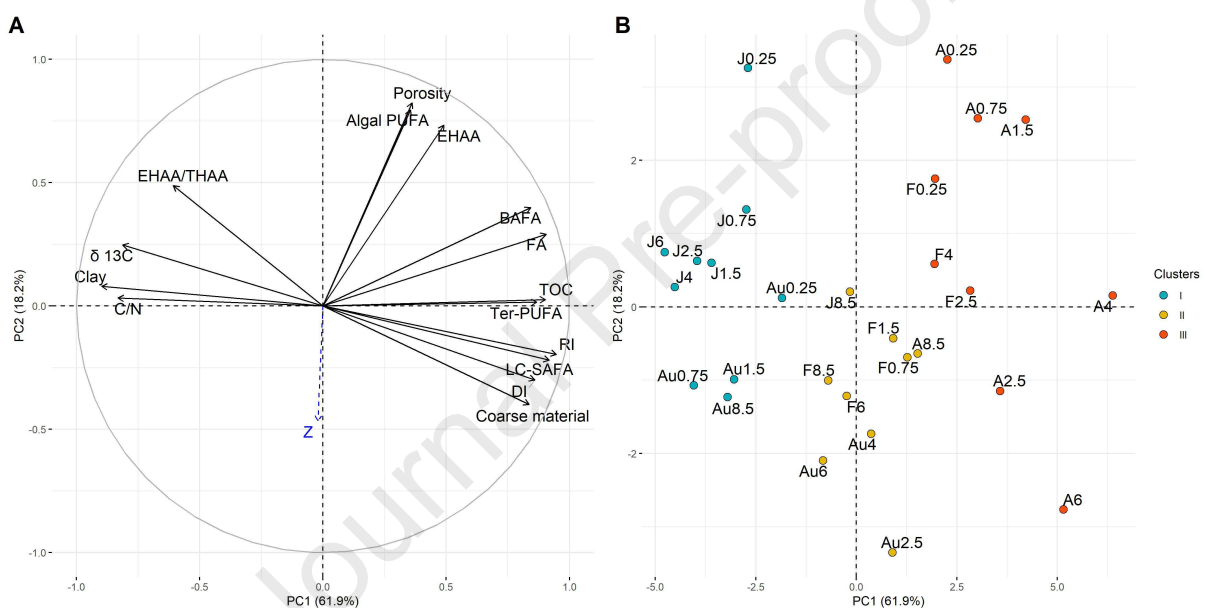
402

403 Figure 4: Principal component analysis (PCA) of sediments collected in the Rhône River prodelta: loading

404 plot (A) and score plot (B) for the first and second principal components (7 sediment layers × 4 dates).

405 Black arrows indicate active variables and the blue arrow corresponds to the supplementary variable

406 (sediment depth: Z). Samples were clustered in 3 groups according to a hierarchical clustering analysis

407 performed on the 5 first principal components of the PCA. Sample code is as follow: the letter

408 indicates the month (F= February, A= April, J= July, Au= August) and the number corresponds to the

409 mid-depth of the sediment layer (in cm). Clay= % of particles <4µm, Coarse material= % of particles

410 >200µm, $CaCO_3$ = % of calcium carbonate. For all other variables see Table 1 for abbreviations.

411 Concentrations in EHAA, fatty acids (FA), BAFA, LC-SAFA, Terrestrial PUFA & Algal PUFA were

412 normalised to organic carbon content.

413

414   Results of the PCA show that sediment properties can be summarised in two independent

415   principal components explaining 80% of the total variance (Fig. 4A). Sediment layers were not

416   grouped by dates or strata on the two first components of the PCA (Fig. 4B), which is consistent with

417   the successive deposition of particles originating from different sources. Two pools of organic inputs

418   were clearly separated on the first component axis (PC1= 61.9 % of the total variance). A group of

419   variables with positive loadings on PC1 characterised a coarser material enriched in TOC, fatty acids,

420   and markers of vascular plants (LC-SAFA and Ter PUFA). This material also exhibited higher DI and RI

421   values, indicative of limited diagenetic alteration, and depleted $\delta^{13}C$ values consistent with an input of

422   modern plant detritus in C3 ($\delta^{13}C$ plant = -28‰, Hedges et al., 1986). Taken together, these results

423   confirm that sediment cores collected in February and April 2010 were enriched in plant detritus (Fig.

424   4B, cluster II). A distinct source of OM associated to clay, low TOC content, higher C/N ratios and $\delta^{13}C$

425   values was found in June and some sediment layers in August 2010 (negative loadings on PC1 and

426   cluster I). OM in the flood deposit (Cluster I) was also more bioavailable for the benthic fauna as seen

427   by higher EHAA/THAA ratios (Fig. 3). The second principal component (PC2= 18.2% of the total

428   variance) illustrates variations that can be attributed to sediment depth, such as the decrease in

429   porosity in the sedimentary column and the rapid degradation of the most labile components (PUFA

430   deriving from phytoplankton and EHAA). The distribution of layers from the April core along PC2

431   agrees with this general pattern: the 2 first centimetres (with positive loadings) being enriched in

432   bioavailable OM, whereas the layers below (with negative loadings) contained a more refractory pool

433   of OM. A second group of samples characterised by lower algal contents and porosity was also linked

434   to PC2. This cluster regroups intermediate layers from August and some layers from February (cluster

435   II on Fig. 4B).

436   The different molecular descriptors used in this study enable to explore the relationships

437   between two fundamental properties of the OM, its origin and its quality. A positive relationship

438   between DI and EHAA/THAA ratio has been previously evidenced supporting the idea that as OM is

439   degraded in the sediments, it becomes less available to enzymes (Dauwe et al., 1999b). Here, the

440 reverse relationship was observed with a significant negative correlation between DI and EHAA/THAA

441 ratio. The mixing of different pools of terrestrial OM may explain these opposite results. A study

442 focusing on the benthic food web in a Mediterranean lagoon has revealed that different types of

443 plants displayed contrasted levels of bioavailability with terrestrial plants exhibiting low EHAA/THAA

444 ratios (10.4-18.1%), seagrasses having intermediary values (12.2-33.4%), and salt marsh vegetation

445 representing a highly digestive source of OM (50.0-60.2%) (Carlier et al., 2007). In good agreement

446 with these earlier results, macrodetritus isolated from sediments at the MESURHO station have a low

447 digestibility (EHAA/THAA ratio = 9.8) and a DI value (0.29) in the range of those calculated for the

448 layers enriched in plant detritus (Pruski, unpublished result). As a general trend bioavailability was thus

449 higher when the contribution of plant detritus was lower (r^2=0.85). Consequently, the lower

450 bioavailability observed in February, April and some layers from August may be attributed to the

451 presence of macrodetritus. There was also a positive correlation between the DI and the proportion of

452 fatty acids specific of epicuticular waxes from leaves (LC-SAFA) indicating that macrodetritus represent

453 in our system a source of fresh OM, and that LC-SAFA are good tracers of litter inputs (i.e. they are less

454 abundant in soils than in the litter).

455   In the flood deposit, soils certainly account for most of the particulate OC exported to the

456 prodelta as observed previously after the flood of June 2008 (Cathalot et al., 2013). This hypothesis is

457 supported by low contributions of biomarkers of phytoplankton and higher plant detritus. The

458 different indexes of degradation provide contrasted insights on the history of this material. The low

459 values of the amino acid based degradation indexes (DI and RI) indicate that the POC exported during

460 the June flood was more degraded than the material delivered during periods of normal river regime

461 (Bourgeois et al., 2011). This is consistent with the weathering of degraded POM from soils or riparian

462 areas during intense rainfall events and the decrease of benthic microbial remineralisation (lower DOU

463 in July and August, Table 2). However, the flood deposit was also characterised by high EHAA/THAA

464 ratios (on average 32% in the flood deposit versus 23% in the February and April cores). The higher

465 bioavailability of this material is somewhat counterintuitive. One would expect soil OM to be less

466 prone to enzymatic digestion than fresh detritus. From this point of view, the particulate matter

467 transferred to the sea during the 2008 and 2010 high-discharge events differed remarkably

468 (EHAA/THAA ~20% in 2008, Bonifácio et al., 2014). In 2008, strong rainfalls were responsible for the

469 opening of the spillway of the Serre Ponçon dam (Marion et al., 2010). Silts were eroded from black

470 marls of the Durance watershed. As a consequence, this material was old and refractory (Δ^{14}C= -

471 495.1‰ ± 1.7 in Cathalot et al., 2013; DI= -0.13, Bourgeois unpublished result). Differences in

472 bioavailability between the TSM delivered during the 2008 and 2010 events may be related to the

473 watersheds affected by the precipitation and the nature of the material transported. Low pigment

474 concentrations in the material exported in June 2010 (Fagervold et al., 2014) indicate that EHAA were

475 mostly associated to non-algal OM, and certainly incorporated to geopolymers as humic substances

476 (Burdige and Martens, 1988). The exported SPM furthermore contained two pools of OM with distinct

477 amino acid compositions: the first and dominant pool was more degraded than the OM delivered

478 during periods of normal discharge (negative DI of the THAAs -0.02±0.03), while another minor

479 fraction of the OM was more labile as shown by elevated DI values calculated on the EHAA (DI_{EHAA}

480 ~0.33± 0.01 for the flood deposit).

481

482 ### 3.5. Temporal changes in meiofaunal community

483 Meiofaunal abundances increased from February (2137 ± 1401 ind. 10 cm^{-2}) to April (9818 ±

484 2027 ind. 10 cm^{-2}) with intermediate abundances in July (6025 ± 1375 ind. 10 cm^{-2}) and August (4574

485 ± 1394 ind. 10 cm^{-2}) (Fig. 5). Nematodes were the most abundant metazoans (70%), followed by

486 harpacticoid copepods (18 %), annelids (4.5%), kinorhynchs (4%), foraminiferans (2%), cumaceans

487 (1%) and turbellarians (0.5%) (Supplementary material, Table S2). This community structure was

488 typical of soft bottom habitats (Danovaro et al., 2000; Giere, 2009; Moodley et al., 2000).

489 Total abundances of meiofauna (Fig. 5) were in the same range as those reported for other

490 sites in the Gulf of Lion (de Bovée et al., 1990; Grémare et al., 2002). Differences between dates were

491   statistically significant (one-way ANOVA, F=15.75, p < 0.001). Pairwise comparisons revealed

492   significantly higher abundances in April and significantly lower in February (Tukey post hoc test,

493   Supplementary material, Tables S3 and S4). The fivefold increase in the meiofaunal abundance from

494   February to April coincided with the inputs of fresh and labile OM on the sea floor (enrichment in algal

495   PUFA and amino acids, Fig. 3). Peaks of abundance are frequently observed after the post-bloom

496   sedimentation of phytodetritus (Palacín et al., 1992; Vanaverbeke et al., 2004). Giere (2009) reported

497   that decaying phytoplankton results in the deposition of a fluffy layer of phytodetritus on the

498   sediment and, after a short time (a few days), those unconsolidated organic deposits enhance the

499   bacterial activity and cause a significant increase in meiofaunal abundance.
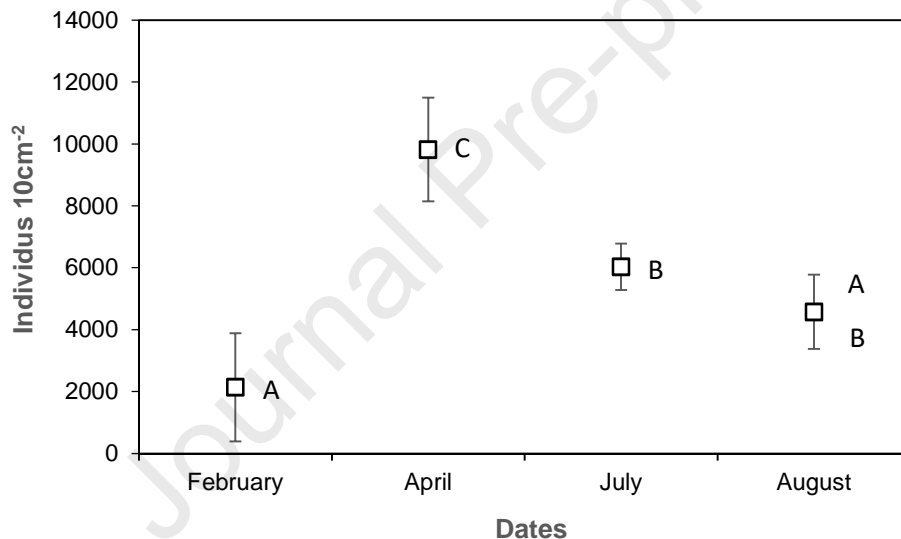
500

501   **Figure 5: Total meiofaunal abundances at the MESURHO station in February, April, July, and August**
502   **2010.** Values are means ± SD (n = 3 cores). Analysis of variance (one-way ANOVA, F=15.75, p < 0.001)
503   and Tukey post hoc test, dates sharing the same letters are not significantly different.

504

505   Results from the two-way ANOVA show the significant effect of sediment depth on the

506   distribution of the meiofauna (F=26.87, p < 0.001). Significant "date x sediment depth" interaction

507   terms (F=3.95; p < 0.001) furthermore indicate that the vertical distribution of the meiofauna differed

508   between sampling periods (Table S5). In February, April and August, the vertical distribution of the

509   meiofauna showed a typical pattern with high abundances near the surface (0-3 cm depth) and

510   decreasing abundances with sediment depth (Fig. 6) as already described by Soetaert et al. (1995) and

511   Vanreusel et al. (1995). The highest values were recorded on the first 2 cm of the cores, which

512   corresponded to the layers of sediment enriched in phytodetritus (Fig. 3). This vertical pattern could

513   be due to the active migration of the meiofauna to the food source accumulated on the sediment

514   surface (Franco et al., 2008; Moens et al., 2013). Sediment oxygenation could be another regulating

515   factor since oxygen penetration in the sediment was very limited in the prodelta area (Fig. 2). Oxic

516   niches were thus only available close to the sediment–water interface.
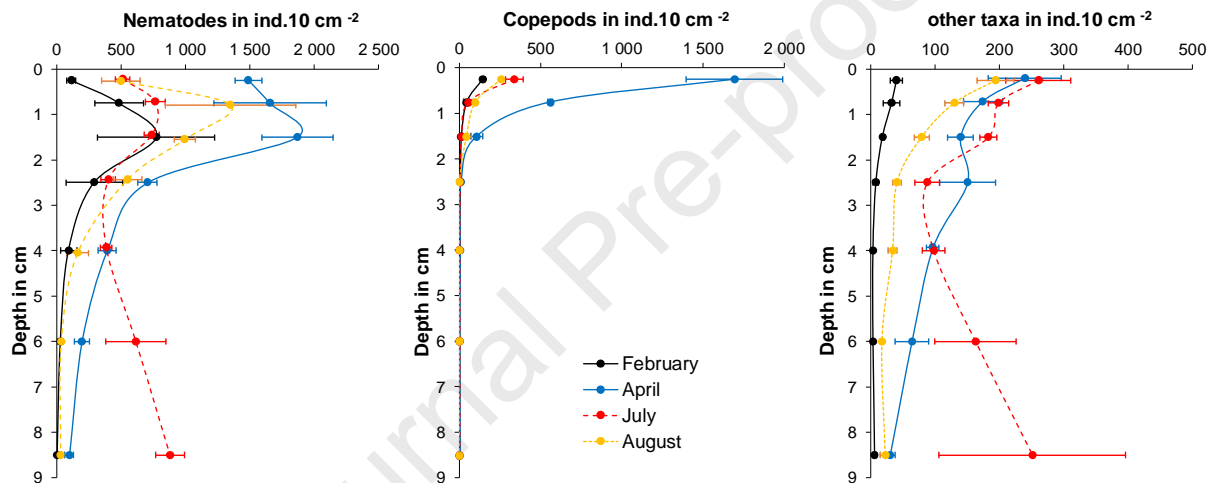
517

518

519   Figure 6: Vertical distribution of meiofauna (nematodes, copepods and other taxa) at the MESURHO

520   station in February, April, July and August 2010. Values are means ± SEM (n=3 cores). Note that some

521   symbols were slightly shifted vertically relative to each other for visibility.

522

523   The vertical distribution of the meiofauna in July differed from the general pattern with high

524   abundances in the deep layers similar to those recorded in the very upper layers of the other dates

525   (two-way ANOVA, p < 0.001, Supplementary material, Table S5). The vertical profiles of copepods

526   seem to fit the pattern of oxygen penetration depth (Fig. 2), but this clearly does not apply to

527   nematodes and foraminiferans, which displayed the highest abundances in deep sediment layers (5 to

528   10 cm depth, Supplementary material, Table S2). These changes in the vertical distribution of the main

529   meiofaunal taxa occurred just a couple of days after the flood of the Rhône tributaries and the sudden

530   increase in TSM (Fig. 1). The drop in meiofaunal total abundance and the presence of a high density of

531   nematodes in the deep layers after this high-discharge event can be explained by the burial of the

532   meiobenthic community as observed experimentally with the simulated deposition of dredged

533   material (Schratzberger et al., 2004). As so the present results corroborate the observation of Pelletier

534   (1999) that high-discharge events severely affect the meiofauna with a reduction of its abundance.

535   Among the "other taxa" the clear dominance of foraminifera from genus *Leptohalysis* was noted in

536   July. This foraminiferan is considered as an opportunistic taxon resistant to high turbidity, large inputs

537   of terrestrially-derived OM, and low oxygen penetration in the sediment (Mojtahid et al., 2009; Scott

538   et al., 2005). An opportunistic strategy allows *Leptohalysis* to proliferate in the Rhône prodelta in just a

539   few days after a flood (Goineau et al., 2012).

540   In August, the community had already recovered a pre-disturbance structure. This short

541   resilience time may be explained by a particularity of the study site. The Gulf of Lion is a highly

542   hydrodynamic system, exposed to frequent strong winds and weather conditions where the benthic

543   ecosystem undergoes frequent physical disturbance (Pont et al., 2002). High hydrodynamism can

544   promote meiofaunal recolonisation. Indeed, while strong currents mechanically remove meiofauna

545   from sediment, the first phases of recolonisation generally proceed very rapidly (1-2 weeks) after a

546   severe devastation (review by Coull and Palmer, 1984; Schratzberger et al., 2004). The rapid dispersal

547   of meiofauna has been ascribed primarily to water column processes, including passive erosion or

548   active emergence (Armonies, 1994, 1988; Palmer et al., 1988; Palmer and Gusf, 1985), but the

549   colonisation of defaunated sediments via lateral interstitial migration has also been observed

550   (Schratzberger et al., 2004).

551

552   3.6. Linking meiofaunal composition and sediment properties

553   Canonical correspondence analysis (CCA) allows to relate the abundance of species to

554   environmental variables (ter Braak, 1986). The canonical ordination diagram summarised the

555 ecological preferences of the meiofaunal taxa at the MESURHO station (Fig. 7). This constrained

556 ordination explained 54% of the total inertia. Permutation tests confirmed that relations between taxa

557 abundances and sediment properties were statistically significant (*p*<0.01) for the sum of all canonical

558 axes (*F* ratio = 2.3) and for the two first axes (*F* ratio = 14.9 and 4.2 for axis 1 and axis 2, respectively).

559 Together, the first and second principal canonical axes accounted for 85% of the relationship between

560 taxa and environmental parameters.
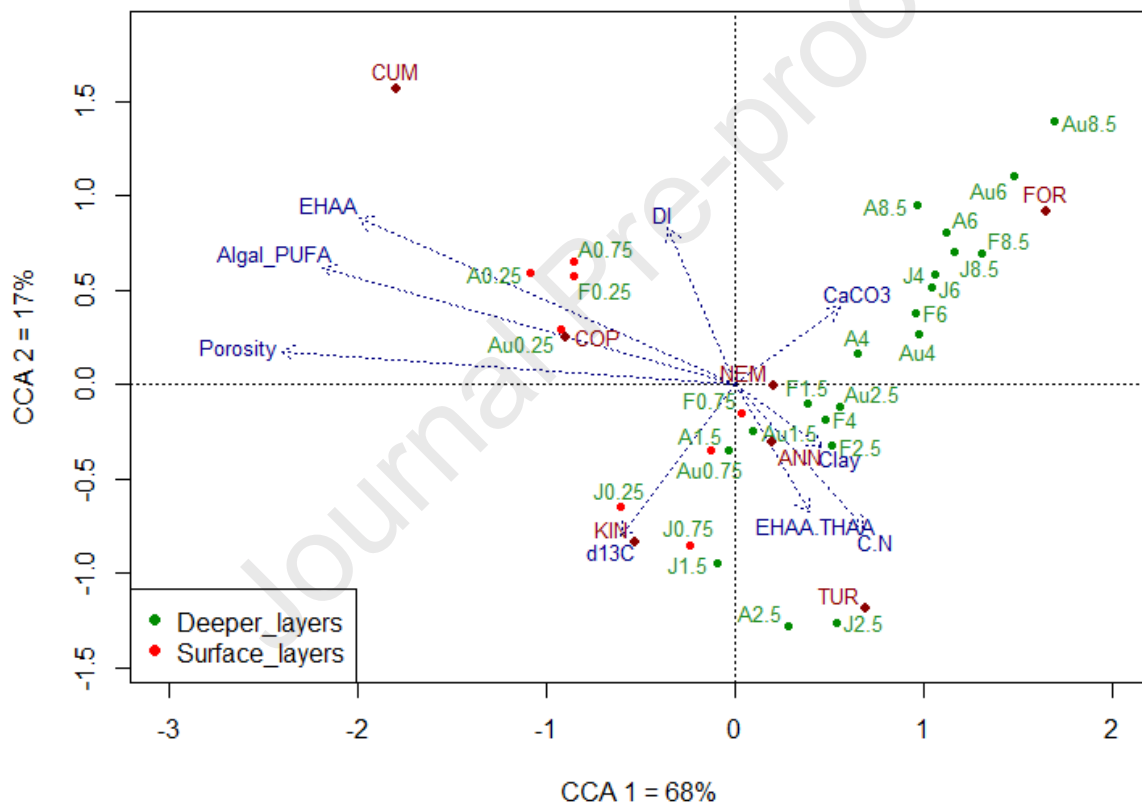
561

562 Figure 7: Canonical correspondence analysis (CCA) triplot showing ordination of meiofaunal taxa at the

563 MESURHO site in February, April, July and August 2010 with environmental variables as arrows and

564 samples as dots.

565 Nematodes (NEM), copepods (COP), kinorhynchs (KIN), annelids (ANN), turbellarians (TUR),

566 cumaceans (CUM), and foraminiferans (FOR). Environmental variables are C/N = molecular carbon to

567 nitrogen ratio, δ^{13}C = bulk stable isotope value, EHAA: normalised concentration in enzymatically

568 hydrolysable amino acids, EHAA/THAA: enzymatically hydrolysable amino acids to total hydrolysable

569   amino acid ratio, DI= degradation index, algal PUFA = normalised concentration in algal

570   polyunsaturated fatty acids, clay= proportion of clay, $CaCO_3$ = calcium carbonate percentage, and

571   porosity.

572   Sample code is as follow: the letter indicates the month (F= February, A= April, J= July, Au= August)

573   and the number corresponds to the mid-depth of the sediment layer (in cm). Red dots indicate surface

574   sediment layers (0-0.5cm and 0.5-1cm), and green dots deeper sediment layers (1-2cm, 2-3cm, 3-5cm,

575   5-7cm, and 7-10cm).

576

577   Among all the candidate environmental constraints, permutation tests showed that porosity,

578   percentage of algal PUFA and normalised concentration of EHAA were the most influential on the

579   meiofauna (Table 3). These three variables were strongly negatively correlated to the first axis,

580   meaning that the main ecological gradient was linked to higher porosity and inputs of labile OM. DI

581   was positively correlated to the second axis, whereas $\delta^{13}C$, C/N and EHAA/THAA were negatively

582   correlated. With no surprise the meiofaunal community was mainly distributed along the first axis

583   according to sediment depth, with negative scores for the surface layers (0-0.5 & 0.5-1 cm) and

584   positive scores for deeper sediments (below 1cm). The meiofauna inhabiting the surface sediments

585   further aggregated on the second axis according to the origin of the OM. As seen before, in February,

586   April and August, fresh suspended particulate matter settled on the seafloor (Fig. 3). The meiofaunal

587   community clearly responded to these inputs of food with higher frequencies of copepods and

588   cumaceans (Fig. 7). A distinct community was found in July in the three first centimetres of the flood

589   deposit. This community was related to higher $\delta^{13}C$, EHAA/THAA, and C/N ratios. Finally, communities

590   from the deepest sediment layers (5-7 and 7-10cm) were grouped and were not related to any of the

591   environmental factors examined in the present study.

592   The constrained ordination also displayed how the meiofaunal taxa were structured with

593   respect to their environmental constraints and agreed well with the known ecological niches of the

594   recorded taxa. Many cumaceans and harpacticoid copepods rely on planktonic diatoms sinking on the

595   seafloor (De Troch et al., 2005; Giere, 2009; Higgins and Thiel, 1988). In good consistency with their

596   feeding habits, cumaceans and copepods were related to inputs of fatty acids produced by

597   phytoplankton and higher level of bioavailable amino acids found on the top of the cores. Kinorhynchs

598   belong to another group with a known preference for the upper (0-3 cm) oxygenated surface layers

599   (Giere, 2009). Shallow water forms feed mainly on diatoms, but they are also linked to organically

600   enriched sediments (Higgins and Thiel, 1988) as those found near river mouths (Guidi-Guilvard and

601   Buscail, 1995). As expected, kinorhynchs were found in the surface sediments, but they displayed high

602   relative frequencies (~13%) in the flood deposit that recovered the seafloor in July. While kinorhynch

603   density in the top layers remained constant from April to August, copepod and cumacean densities

604   dropped remarkably after the flood (Supplementary material, Table S2). This shows that crustaceans

605   and kinorhynchs respond differently to river regime. In a mesocosm study, Rudnick (1989) found that

606   copepods and kinorhynchs belong to two distinct feeding groups; the first group consuming fresh OM,

607   while the second one could use older detrital matter. However, since the sampling only occurred a

608   few days after the flood, it seems unlikely that the nature of the available OM could be the factor

609   affecting meiofaunal community in July. Kinorhynchs can perform vertical movements in the sediment

610   (Shimanaga et al., 2000). A higher capacity to migrate upward and colonise the newly flood deposit

611   could explain the apparent resilience of kinorhynchs to the physical perturbation induced by the high-

612   discharge event. Nematodes and annelids were the taxa whose occurrence and variability in density

613   were the less explained by the CCA. Free-living nematodes, the metazoans with the greatest species

614   richness in the sediments, occupy various ecological niches with different trophic requirements and

615   sediment preferences (Giere, 2009; Moens et al., 2013), which may explain their wide vertical

616   distribution. The ordination showed anyway their preference for subsurface and deeper sediment

617   layers. Like nematodes, meiobenthic annelids are euryoecious, their preferences relate to sediment

618   structure and organic content (Giere, 2009; Villora-Moreno, 1997). In the present study, they were

619   related to ascending EHAA/THAA and C/N ratios. Foraminiferans were associated with deeper

620   sediment layers and $CaCO_3$. Most foraminiferans are versatile for microhabitat selection, food supply

621   and oxygen availability. Mojtahid et al. (2010) investigated microhabitat preferences of living

622   foraminiferans in front of the Rhône River mouth. They found two different assemblages: infaunal

623   species with maximum densities in anoxic layers were dominant close to the river mouth, while

624   species living predominantly in the top surface layer dominated in areas less influenced by fluvial

625   inputs. They postulated that the higher tolerance of infaunal species for degraded terrestrial OM

626   explains their dominance in the prodelta area. This is consistent with the CCA ordination showing that

627   foraminiferans were related to rather low δ^{13}C (meaning higher contribution of terrestrial OM). Finally,

628   turbellarians, a group with predatory habits or feeding on diatoms, only occurred in two samples

629   (layers 2-3 cm in April and July). Hence, little can be said of their ecological optimum. However, their

630   occurrence is generally determined by the sediment water and oxygen contents (Giere, 2009).

631   The CCA highlighted that the main ecological gradients for the meiofaunal community in the

632   Rhône prodelta were related to sediment depth and river regime. Strong vertical patterns are found in

633   recent sediments with the degradation of the most labile organic components and short-scale

634   variations of abiotic parameters (oxygenation, redox potential…). These vertical patterns constrain the

635   distribution of the meiofauna (Maria et al., 2012). In contrast, river regime accounts for temporal

636   changes in the amount, provenance and nature of the OM accumulated in the prodelta (Cathalot et

637   al., 2010). The relationships between the meiofauna and the biochemical characteristics of

638   sedimentary OM have been previously investigated by de Bovée et al. (1990) and Grémare et al.

639   (2002) in the Gulf of Lion. They reported that meiofaunal abundance correlated better with

640   concentrations in lipids and EHAA rather than with bulk properties of the OM (nitrogen and organic

641   carbon contents) on the shelf (0 – 175 m depth range). In the present study, porosity, algal PUFA and

642   EHAA were the best predictors of meiofaunal composition, whereas porosity, δ^{13}C and DI was the best

643   combination of explanatory variables (Table 3). The strong influence of porosity on the meiofauna is

644   certainly indirect. This factor is related to sediment depth as many other environmental variables not

645   measured in the present study. In particular, porosity partially controls important abiotic factors such

646   as dissolved oxygen diffusion and thus redox potential (Eh). The present results furthermore show that

647   qualitative descriptors of sedimentary organics not only explain spatiotemporal changes in meiofaunal

648   composition (de Bovée et al., 1990; Grémare et al., 2002), but also temporal changes in the vertical

649   distribution of meiofaunal taxa.

650

651   4. Conclusions

652   Major variations of the origin and quality of sedimentary OM are observed in the Rhône River

653   prodelta at a monthly time scale. These fluctuations are mainly controlled by the fast dynamic of the

654   processes affecting river flow and inputs from the watershed, but also by biological and physical

655   processes in the coastal area. Terrestrial organic inputs exported mostly during periods of high river

656   discharge are preserved in the sediments until further remobilisation (Fig. 8). High-discharge events in

657   autumn and winter mostly bring a material enriched in plant detritus, while other events as the one

658   triggered by intense rainfalls in June 2010 are responsible for the transport of more degraded and

659   poorly reactive POC. These different pools of OM (soil, litter, phytodetritus), with variable composition

660   and quality, constitute a variety of trophic resources for the infauna. In this very complex and dynamic

661   system, the meiofaunal community is driven by both trophic conditions and deposition of new

662   sediment layers linked to the hydrological regime of the Rhône River. Inputs of high quality OM

663   (highlighted by fatty acid biomarkers and amino acid indices) appear as a key structuring factor for the

664   meiofauna as already showed by Vanreusel et al. (1995) and Giere (2009). Meiofauna is more

665   abundant in spring when the sedimentation of labile OM originating from the phytoplankton bloom

666   induced eutrophic conditions, whereas meiofaunal densities are low in late summer due to reduced

667   inputs of labile POC (Fig. 8). The current results also point out the rapid response of the meiofauna to

668   a short high-discharge event and the higher importance of analysing the vertical distribution of

669   meiofaunal taxa rather than the total meiofauna abundances, since it was more relevant to show the

670   perturbation. The meiofauna was severely impacted by this physical disturbance with a significant

671   decrease of its total density and the burial of the meiobenthic community under the flood deposit,

672   even though the newly settled layer was rapidly colonised (less than 2 months). The fast recovery of

673   the meiobenthic community highlights that the meiofauna accounts for a highly resilient component

674   of the benthic ecosystem in the vicinity of the Rhône River mouth, in contrast to the macrofauna,

675   which is much longer affected by high-discharge events (Bonifácio et al., 2014).
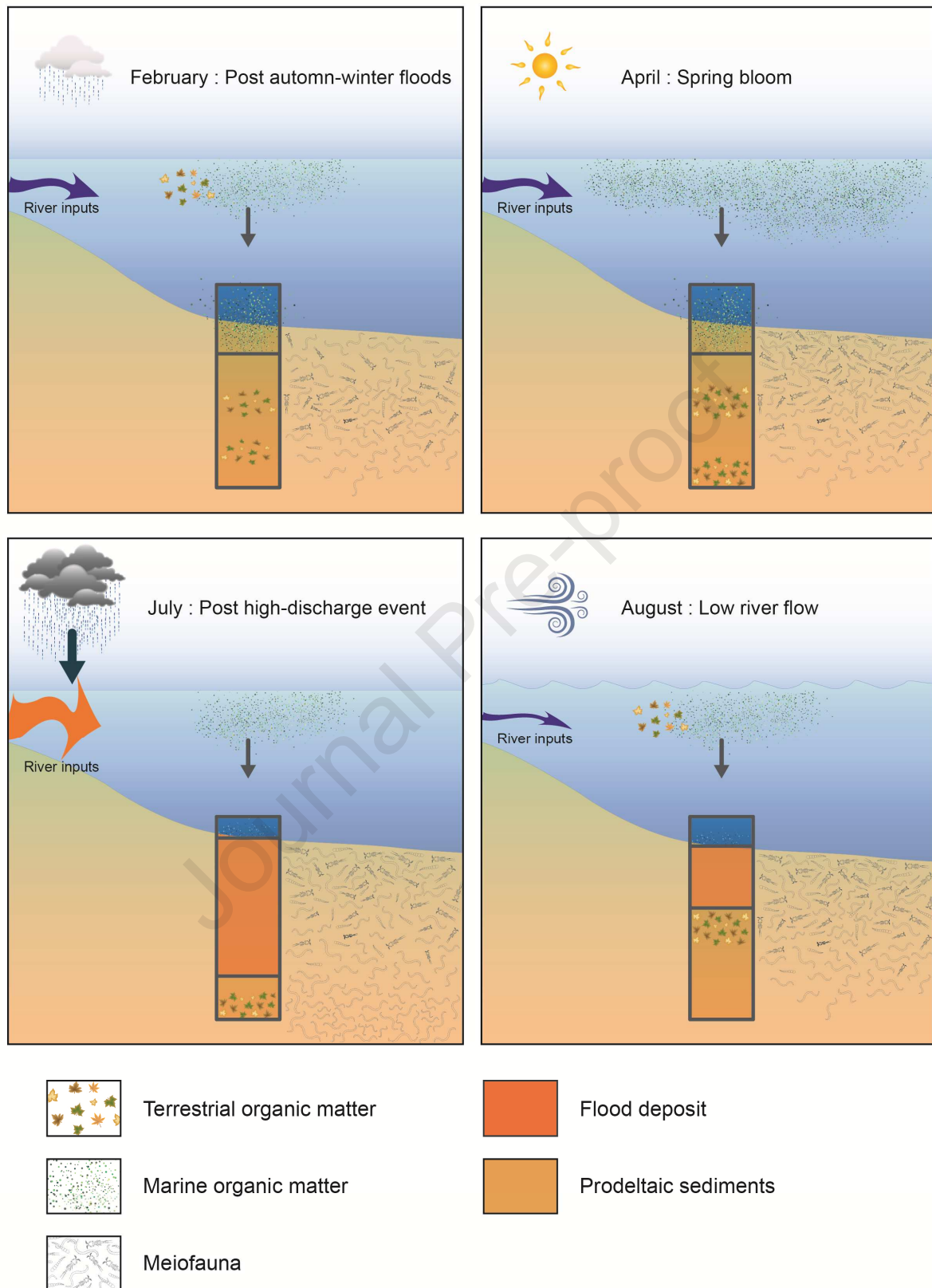
Figure 8: Synthetic scheme of the processes influencing the dynamic of organic matter and meiofaunal community composition during the four investigated periods in the Rhône prodelta.

679

680   5. Acknowledgements

690   References

691   Akoumianaki, I., Nicolaidou, A., 2007. Spatial variability and dynamics of macrobenthos in a

692   Mediterranean delta front area: The role of physical processes. Journal of Sea Research 57,

693   47–64. https://doi.org/10.1016/j.seares.2006.07.003

694   Akoumianaki, I., Papaspyrou, S., Kormas, K.Ar., Nicolaidou, A., 2013. Environmental variation and

695   macrofauna response in a coastal area influenced by land runoff. Estuarine, Coastal and Shelf

696   Science, Estuarine and lagoon biodiversity and their natural goods and services 132, 34–44.

697   https://doi.org/10.1016/j.ecss.2012.04.009

698   Akoumianaki, I., Papaspyrou, S., Nicolaidou, A., 2006. Dynamics of macrofaunal body size in a deltaic

699   environment.   Marine   Ecology   Progress   Series   321,   55–66.

700   https://doi.org/10.3354/meps321055

701   Alkhatib, M., Schubert, C.J., del Giorgio, P.A., Gélinas, Y., Lehmann, M.F., 2012. Organic matter

702   reactivity indicators in sediments of the St. Lawrence Estuary. Estuarine, Coastal and Shelf

703   Science 102–103, 36–47. https://doi.org/10.1016/j.ecss.2012.03.002

704   Antonelli, C., Eyrolle, F., Rolland, B., Provansal, M., Sabatier, F., 2008. Suspended sediment and 137Cs

705   fluxes during the exceptional December 2003 flood in the Rhône River, southeast France.

706   Geomorphology 95, 350–360. https://doi.org/10.1016/j.geomorph.2007.06.007

707   Armonies, W., 1994. Drifting meio- and macrobenthic invertebrates on tidal flats in Königshafen: A

708   review. Helgolander Meeresunters 48, 299–320. https://doi.org/10.1007/BF02367043

709   Armonies, W., 1988. Active emergence of meiofauna from intertidal sediment. Marine Ecology

710   Progress Series 43, 151–159. https://doi.org/10.3354/meps043151

711   Balsamo, M., Semprucci, F., Frontalini, F., Coccioni, R., 2012. Meiofauna as a tool for marine

712   ecosystem   biomonitoring,   in: Marine   Ecosystems.   In   Tech,   pp.   77–104.

713   https://doi.org/10.5772/34423

714   Bauer, J.E., Cai, W.-J., Raymond, P.A., Bianchi, T.S., Hopkinson, C.S., Regnier, P.A.G., 2013. The

715   changing   carbon   cycle   of   the   coastal   ocean.   Nature   504,   61–70.

716   https://doi.org/10.1038/nature12857

717   Berner, R.A., 1980. Early diagenesis: A theoretical approach. Princeton Univ Pr.

718   Besset, M., Anthony, E.J., Sabatier, F., 2017. River delta shoreline reworking and erosion in the

719   Mediterranean and Black Seas: the potential roles of fluvial sediment starvation and other

720   factors. Elementa: Science of the Anthropocene 5, 54. https://doi.org/10.1525/elementa.139

721   Bianchi, T.S., Allison, M.A., 2009. Large-river delta-front estuaries as natural "recorders" of global

722   environmental change. Proceedings of the National Academy of Sciences 106, 8085–8092.

723   https://doi.org/10.1073/pnas.0812878106

724   Bianchi, T.S., Canuel, E.A., 2011. Chapter 2. Chemical biomarkers applications to ecology and

725   paleoecology, in: Chemical Biomarkers in Aquatic Ecosystems. Princeton University Press, pp.

726   19–29.

727   Blanchet, F.G., Legendre, P., Borcard, D., 2008. Forward selection of explanatory variables. Ecology 89,

728   2623–2632. https://doi.org/10.1890/07-0986.1

729   Bonifácio, P., Bourgeois, S., Labrune, C., Amouroux, J.M., Escoubeyrou, K., Buscail, R., Romero-

730   Ramirez, A., Lantoine, F., Vétion, G., Bichon, S., Desmalades, M., Rivière, B., Deflandre, B.,

731   Grémare, A., 2014. Spatiotemporal changes in surface sediment characteristics and benthic

732   macrofauna composition off the Rhône River in relation to its hydrological regime. Estuarine,

733   Coastal and Shelf Science 151, 196–209. https://doi.org/10.1016/j.ecss.2014.10.011

734   Borcard, D., Gillet, F., Legendre, P., 2011. Numerical ecology with R, Use R! Springer, New York.

735   Boudreau, B.P., Jorgensen, B.B., 2001. The Benthic boundary layer: transport processes and

736   biogeochemistry. Oxford University Press.

737   Bourgeois, S., Pruski, A.M., Sun, M.-Y., Buscail, R., Lantoine, F., Kerhervé, P., Vétion, G., Rivière, B.,

738   Charles, F., 2011. Distribution and lability of land-derived organic matter in the surface

739   sediments of the Rhône prodelta and the adjacent shelf (Mediterranean Sea, France): a multi

740   proxy study. Biogeosciences 8, 3107–3125. https://doi.org/10.5194/bg-8-3107-2011

741 Broecker, W., Peng, T., 1974. Gas-Exchange Rates Between Air and Sea. Tellus 26, 21–35.

742   https://doi.org/10.1111/j.2153-3490.1974.tb01948.x

743 Budge, S.M., Parrish, C.C., McKenzie, C.H., 2001. Fatty acid composition of phytoplankton, settling

744   particulate matter and sediments at a sheltered bivalve aquaculture site. Marine Chemistry

745   76, 285–303.

746 Burdige, D.J., Martens, C.S., 1988. Biogeochemical cycling in an organic-rich coastal marine basin: 10.

747   The role of amino acids in sedimentary carbon and nitrogen cycling. Geochimica et

748   Cosmochimica Acta 52, 1571–1584. https://doi.org/10.1016/0016-7037(88)90226-8

749 Cai, W., Reimers, C., 1993. The Development of Ph and Pco2 Microelectrodes for Studying the

750   Carbonate Chemistry of Pore Waters Near the Sediment-Water Interface. Limnol. Oceanogr.

751   38, 1762–1773. https://doi.org/10.4319/lo.1993.38.8.1762

752 Cardoso, P.G., Raffaelli, D., Lillebø, A.I., Verdelhos, T., Pardal, M.A., 2008. The impact of extreme

753   flooding events and anthropogenic stressors on the macrobenthic communities' dynamics.

754   Estuarine, Coastal and Shelf Science, Submarine groundwater discharge studies along the

755   Ubatuba   coastal   area   in   south-eastern   Brazil   76,   553–565.

756   https://doi.org/10.1016/j.ecss.2007.07.026

757 Carlier, A., Riera, P., Amouroux, J.-M., Bodiou, J.-Y., Escoubeyrou, K., Desmalades, M., Caparros, J.,

758   Grémare, A., 2007. A seasonal survey of the food web in the Lapalme Lagoon (northwestern

759   Mediterranean) assessed by carbon and nitrogen stable isotope analysis. Estuarine, Coastal

760   and Shelf Science 73, 299–315. https://doi.org/10.1016/j.ecss.2007.01.012

761 Cathalot, C., Rabouille, C., Pastor, L., Deflandre, B., Viollier, E., Buscail, R., Grémare, A., Treignier, C.,

762   Pruski, A., 2010. Temporal variability of carbon recycling in coastal sediments influenced by

763   rivers: assessing the impact of flood inputs in the Rhône River prodelta. Biogeosciences 7,

764   1187–1205.

765   Cathalot, C., Rabouille, C., Tisnerat-Laborde, N., Toussaint, F., Kerherve, P., Buscail, R., Loftis, K., Sun,

766   M.-Y., Tronczynski, J., Azoury, S., Lansard, B., Treignier, C., Pastor, L., Tesi, T., 2013. The fate of

767   river organic carbon in coastal areas: A study in the Rhone River delta using multiple isotopic

768   (delta C-13, Delta C-14) and organic tracers. Geochimica et Cosmochimica Acta 118, 33–55.

769   https://doi.org/10.1016/j.gca.2013.05.001

770   Copard, Y., Eyrolle, F., Radakovitch, O., Poirel, A., Raimbault, P., Gairoard, S., Di-Giovanni, C., 2018.

771   Badlands as a hot spot of petrogenic contribution to riverine particulate organic carbon to the

772   Gulf of Lion (NW Mediterranean Sea). Earth Surface Processes and Landforms 43, 2495–2509.

773   https://doi.org/10.1002/esp.4409

774   Coull, B.C., 1999. Role of meiofauna in estuarine soft-bottom habitats. Austral Ecology 24, 327–343.

775   https://doi.org/10.1046/j.1442-9993.1999.00979.x

776   Coull, B.C., 1990. Are Members of the Meiofauna Food for Higher Trophic Levels? Transactions of the

777   American Microscopical Society 109, 233–246. https://doi.org/10.2307/3226794

778   Coull, B.C., Chandler, G.T., 1992. Pollution and meiofauna: field, laboratory, and mesocosm studies.

779   Oceanography and Marine Biology: An Annual Review 30, 191–271.

780   Coull, B.C., Palmer, M.A., 1984. Field experimentation in meiofaunal ecology. Hydrobiologia 118, 1–19.

781   https://doi.org/10.1007/BF00031783

782   Danovaro, R., Gambi, C., Manini, E., Fabiano, M., 2000. Meiofauna response to a dynamic river plume

783   front. Marine Biology 137, 359–370. https://doi.org/10.1007/s002270000353

784   Dauwe, B., Middelburg, J.J., Herman, P.M.J., Heip, C.H.R., 1999a. Linking diagenetic alteration of amino

785   acids and bulk organic matter reactivity. Limnology and Oceanography 44, 1809–1814.

786   Dauwe, B., Middelburg, J.J., Van Rijswijk, P., Sinke, J., Herman, P.M.J., Heip, C.H.R., 1999b.

787   Enzymatically hydrolyzable amino acids in North Sea sediments and their possible implication

788   for sediment nutritional values. Journal of Marine Research 57, 109–134.

789   Day, J.W., Ibáñez, C., Pont, D., Scarton, F., 2019a. Chapter 14 - Status and Sustainability of

790   Mediterranean Deltas: The Case of the Ebro, Rhône, and Po Deltas and Venice Lagoon, in:

791   Wolanski, E., Day, J.W., Elliott, M., Ramachandran, R. (Eds.), Coasts and Estuaries. Elsevier, pp.

792   237–249. https://doi.org/10.1016/B978-0-12-814003-1.00014-9

793   Day, J.W., Ramachandran, R., Giosan, L., Syvitski, J., Paul Kemp, G., 2019b. Chapter 9 - Delta Winners

794   and Losers in the Anthropocene, in: Wolanski, E., Day, J.W., Elliott, M., Ramachandran, R.

795   (Eds.), Coasts and Estuaries. Elsevier, pp. 149–165. https://doi.org/10.1016/B978-0-12-

796   814003-1.00009-5

797   de Bovée, F., Guidi, L.D., Soyer, J., 1990. Quantitative distribution of deep-sea meiobenthos in the

798   northwestern Mediterranean (Gulf of Lions). Continental Shelf Research 10, 1123–1145.

799   https://doi.org/10.1016/0278-4343(90)90077-Y

800   De Troch, M., Steinarsdottir, M., Chepurnov, V., Olafsson, E., 2005. Grazing on diatoms by harpacticoid

801   copepods: species-specific density-dependent uptake and microbial gardening. Aquatic

802   Microbial Ecology 39, 135–144.

803   Dufois, F., Verney, R., Le Hir, P., Dumas, F., Charmasson, S., 2014. Impact of winter storms on sediment

804   erosion in the Rhone River prodelta and fate of sediment in the Gulf of Lions (North Western

805   Mediterranean Sea). Continental Shelf Research 72, 57–72.

806   https://doi.org/10.1016/j.csr.2013.11.004

807   Dunstan, G.A., Volkman, J.K., Barrett, S.M., Leroi, J.M., Jeffrey, S.W., 1994. Essential polyunsaturated

808   fatty acids from 14 species of diatom (Bacillariophyceae). Phytochemistry 35, 155–161.

809   Fagervold, S.K., Bourgeois, S., Pruski, A.M., Charles, F., Kerhervé, P., Vetion, G., Galand, P.E., 2014.

810   River organic matter shapes microbial communities in the sediment of the Rhône prodelta.

811   The ISME journal. https://doi.org/10.1038/ismej.2014.86

812   Fontanier, C., Jorissen, F., Lansard, B., Mouret, A., Buscail, R., Schmidt, S., Kerherve, P., Buron, F.,

813   Zaragosi, S., Hunault, G., Ernoult, E., Artero, C., Anschutz, P., Rabouille, C., 2008. Live

814   foraminifera from the open slope between Grand Rhone and Petit Rhone Canyons (Gulf of

815   Lions, NW Mediterranean). Deep Sea Research Part I: Oceanographic Research Papers 55,

816   1532–1553. https://doi.org/10.1016/j.dsr.2008.07.003

817   Franco, M.A., Soetaert, K., Oevelen, D.V., Gansbeke, D.V., Costa, M.J., Vincx, M., Vanaverbeke, J., 2008.

818   Density, vertical distribution and trophic responses of metazoan meiobenthos to

819   phytoplankton deposition in contrasting sediment types. Marine Ecology Progress Series 358,

820   51–62. https://doi.org/10.3354/meps07361

821   Franzo, A., Asioli, A., Roscioli, C., Patrolecco, L., Bazzaro, M., Del Negro, P., Cibic, T., 2019. Influence of

822   natural and anthropogenic disturbances on foraminifera and free-living nematodes in four

823   lagoons of the Po delta system. Estuarine, Coastal and Shelf Science 220, 99–110.

824   https://doi.org/10.1016/j.ecss.2019.02.039

825   Gambi, C., Totti, C., Manini, E., 2003. Impact of Organic Loads and Environmental Gradients on

826   Microphytobenthos and Meiofaunal Distribution in a Coastal Lagoon. Chemistry and Ecology

827   19, 207–223. https://doi.org/10.1080/0275754031000119951

828   Gee, J.M., 1989. An ecological and economic review of meiofauna as food for fish. Zoological Journal

829   of The Linnean Society 96, 243–261. https://doi.org/10.1111/j.1096-3642.1989.tb02259.x

830   Giere, O., 2009. Meiobenthology: The Microscopic Motile Fauna of Aquatic Sediments, 2nd ed.

831   Springer-Verlag, Berlin Heidelberg. https://doi.org/10.1007/978-3-540-68661-3

832   Giosan, L., Syvitski, J., Constantinescu, S., Day, J., 2014. Climate change: Protect the world's deltas.

833   Nature News 516, 31. https://doi.org/10.1038/516031a

834   Goineau, A., Fontanier, C., Jorissen, F., Buscail, R., Kerherve, P., Cathalot, C., Pruski, A.M., Lantoine, F.,

835   Bourgeois, S., Metzger, E., Legrand, E., Rabouille, C., 2012. Temporal variability of live (stained)

836   benthic foraminiferal faunas in a river-dominated shelf - Faunal response to rapid changes of

837   the river influence (Rhone prodelta, NW Mediterranean). Biogeosciences 9, 1367–1388.

838   https://doi.org/10.5194/bg-9-1367-2012

839   Grémare, A., Medernach, L., deBovee, F., Amouroux, J.M., Vetion, G., Albert, P., 2002. Relationships

840   between sedimentary organics and benthic meiofauna on the continental shelf and the upper

841   slope of the Gulf of Lions (NW Mediterranean). Marine Ecology Progress Series 234, 85–94.

842   Guidi-Guilvard, L.D., Buscail, R., 1995. Seasonal survey of metazoan meiofauna and surface sediment

843   organics in a non-tidal turbulent sublittoral prodelta (northwestern Mediterranean).

844   Continental Shelf Research 15, 633–653. https://doi.org/10.1016/0278-4343(94)E0036-L

845   Harmelin-Vivien, M., Dierking, J., Bănaru, D., Fontaine, M.F., Arlhac, D., 2010. Seasonal variation in

846   stable C and N isotope ratios of the Rhone River inputs to the Mediterranean Sea (2004–

847   2005). Biogeochemistry 100, 139–150. https://doi.org/10.1007/s10533-010-9411-z

848   Harmelin-Vivien, M., Loizeau, V., Mellon, C., Beker, B., Arlhac, D., Bodiguel, X., Ferraton, F., Hermand,

849   R., Philippon, X., Salen-Picard, C., 2008. Comparison of C and N stable isotope ratios between

850   surface particulate organic matter and microphytoplankton in the Gulf of Lions (NW

851   Mediterranean). Continental Shelf Research 28, 1911–1919.

852   https://doi.org/10.1016/j.csr.2008.03.002

853   Hedges, J.I., Clark, W.A., Quay, P.D., Richey, J.E., Devol, A.H., Santos, U. de M., 1986. Compositions and

854   fluxes of particulate organic material in the Amazon River. Limnology and Oceanography 31,

855   717–738.

856   Hedges, J.I., Oades, J.M., 1997. Comparative organic geochemistries of soils and marine sediments.

857   Organic Geochemistry 27, 319–361. https://doi.org/10.1016/S0146-6380(97)00056-9

858   Heip, C.H.R., Vincx, M., Vranken, G., 1985. The ecology of marine nematodes. Oceanography and

859   Marine Biology: An Annual Review.

860   Hermand, R., Salen-Picard, C., Alliot, E., Degiovanni, C., 2008. Macrofaunal density, biomass and

861   composition of estuarine sediments and their relationship to the river plume of the Rhône

862   River (NW Mediterranean). Estuarine, Coastal and Shelf Science 79, 367–376.

863   Higgins, R.P., Thiel, H., 1988. Introduction to the study of meiofauna, illustrée, révisée, réimprimée. ed.

864   Smithsonian Institution Press, University of Maine.

865   Higueras, M., Kerhervé, P., Sanchez-Vidal, A., Calafat, A., Ludwig, W., Verdoit-Jarraya, M., Heussner, S.,

866   Canals, M., 2014. Biogeochemical characterization of the riverine particulate organic matter

867   transferred to the NW Mediterranean Sea. Biogeosciences 11, 157–172.

868   https://doi.org/10.5194/bg-11-157-2014

869   Husson, F., Josse, J., Pages, J., 2010. Principal component methods-hierarchical clustering-partitional

870   clustering: why would we need to choose for visualizing data? Applied Mathematics

871   Department.

872   Jennerjahn, T.C., Ittekkot, V., 1997. Organic matter in sediments in the mangrove areas and adjacent

873   continental margins of Brazil: I. Amino acids and hexosamines. Oceanologica Acta 20, 359–

874   369.

875   Lansard, B., Rabouille, C., Denis, L., Grenz, C., 2008. In situ oxygen uptake rates by coastal sediments

876   under the influence of the Rhone River (NW Mediterranean Sea). Continental Shelf Research

877   28, 1501–1510. https://doi.org/10.1016/j.csr.2007.10.010

878   Lê, S., Josse, J., Husson, F., 2008. FactoMineR: An R Package for Multivariate Analysis | Lê | Journal of

879   Statistical Software 25, 1–18. https://doi.org/10.18637/jss.v025.i01

880   Leithold, E.L., Hope, R.S., 1999. Deposition and modification of a flood layer on the northern California

881   shelf: lessons from and about the fate of terrestrial particulate organic carbon. Marine

882   Geology 154, 183–195.

883   Li, Y., Gregory, S., 1974. Diffusion of Ions in Sea-Water and in Deep-Sea Sediments. Geochimica et

884   Cosmochimica Acta 38, 703–714.

885   Lindroth, P., Mopper, K., 1979. High performance liquid chromatographic determination of

886   subpicomole amounts of amino acids by precolumn fluorescence derivatization with ortho-

887   phthaldialdehyde. Analytical Chemistry 51, 1667–1674.

888   Lohrer, A.M., Thrush, S.F., Hewitt, J.E., Berkenbusch, K., Ahrens, M., Cummings, V.J., 2004. Terrestrially

889   derived sediment: response of marine macrobenthic communities to thin terrigenous

890   deposits. Marine Ecology Progress Series 273, 121–138. https://doi.org/10.3354/meps273121

891   Lorthiois, T., 2012. Dynamique des matières en suspension dans le panache du Rhône (Méditerranée

892   occidentale) par télédétection spatiale "couleur de l'océan" (thesis). Université Paris 6.

893   Maillet, G.M., Vella, C., Berné, S., Friend, P.L., Amos, C.L., Fleury, T.J., Normand, A., 2006.

894   Morphological changes and sedimentary processes induced by the December 2003 flood

895   event at the present mouth of the Grand Rhône River (southern France). Marine Geology 234,

896   159–177.

897   Maria, T.F., Vanaverbeke, J., Esteves, A.M., De Troch, M., Vanreusel, A., 2012. The importance of

898   biological interactions for the vertical distribution of nematodes in a temperate ultra-

899   dissipative sandy beach. Estuarine, Coastal and Shelf Science 97, 114–126.

900   https://doi.org/10.1016/j.ecss.2011.11.030

901   Marion, C., Maillet, G., Arnaud, M., Eyrolle, F., 2010. Quantifications des flux solides rhôdaniens à

902   l'embouchure: apports de la Durance pendant la crue exceptionnelle de mai 2008. La Houille

903   Blanche 72–80. https://doi.org/10.1051/lhb/2010057

904   Martin, D., Pititto, F., Gil, J., Mura, M.P., Bahamon, N., Romano, C., Thorin, S., Schvartz, T., Dutrieux, É.,

905   Bocquenet, Y., 2019. Long-distance influence of the Rhône River plume on the marine benthic

906   ecosystem: Integrating descriptive ecology and predictive modelling. Science of The Total

907   Environment 673, 790–809. https://doi.org/10.1016/j.scitotenv.2019.04.010

908   Mayer, L.M., Schick, L.L., Sawyer, T., Plante, C.J., Jumars, P.A., Self, R.L., 1995. Bioavailable amino acids

909   in sediments: a biomimetic, kinetics-based approach. Limnology and Oceanography 40, 511–

910   520.

911   Meyers, P.A., 1997. Organic geochemical proxies of paleoceanographic, paleolimnologic, and

912   paleoclimatic processes. Organic Geochemistry 27, 213–250.

913   Moens, T., Braeckman, U., Derycke, S., Fonseca, G., Gallucci, F., Ingels, J., Leduc, D., Vanaverbeke, J.,

914   Van Colen, C., Vanreusel, A., Vincx, M., 2013. Ecology of free-living marine nematodes, in:

915   Handbook of Zoology: Gastrotricha, Cycloneuralia and Gnathifera, Vol. 2 : Nematoda. De

916   Gruyter, pp. 109–152.

917   Mojtahid, M., Jorissen, F., Lansard, B., Fontanier, C., 2010. Microhabitat selection of benthic
918   foraminifera in sediments off the Rhöne River mouth (NW Mediterranean). Journal of
919   Foraminiferal Research 40, 231–246. https://doi.org/10.2113/gsjfr.40.3.231
920   Mojtahid, M., Jorissen, F., Lansard, B., Fontanier, C., Bombled, B., Rabouille, C., 2009. Spatial
921   distribution of live benthic foraminifera in the Rhône prodelta: faunal response to a
922   continental-marine organic matter gradient. Marine Micropaleontology 70, 177–200.
923   https://doi.org/10.1016/j.marmicro.2008.12.006
924   Moloney, C.L., Field, J.G., 1991. The size-based dynamics of plankton food webs. I. A simulation model
925   of carbon and nitrogen flows. Journal of Plankton Research 13, 1003–1038.
926   https://doi.org/10.1093/plankt/13.5.1003
927   Moodley, L., Chen, G., Heip, C.H.R., Vincx, M., Ecosystems Studies, 2000. Vertical distribution of
928   meiofauna in sediments from contrasting sites in the Adriatic Sea: Clues to the role of abiotic
929   versus   biotic   control.   Ophelia   53,   203–212.
930   https://doi.org/10.1080/00785326.2000.10409450
931   Motoda, S., 1959. Devices of simple plankton apparatus. Memoirs of the Faculty of Fisheries, Hokkaido
932   University, 7(1-2), 73-9.
933   Norkko, A., Thrush, S.F., Hewitt, J.E., Cummings, V.J., Norkko, J., Ellis, J.I., Funnell, G.A., Schultz, D.,
934   MacDonald, I., 2002. Smothering of estuarine sandflats by terrigenous clay: the role of wind-
935   wave disturbance and bioturbation in site-dependent macrofaunal recovery. Marine Ecology
936   Progress Series 234, 23–42. https://doi.org/10.3354/meps234023
937   Oksanen, J., Blanchet, F.G., Friendly, M., Kindt, R., Legendre, P., McGlinn, D., Minchin, P.R., O'Hara,
938   R.B., Simpson, G.L., Solymos, P., Henry, M., Stevens, H., E Szoecs, Wagner, H., 2016. vegan:
939   Community Ecology Package. CRAN: The Comprehensive R Archive Network.
940   O'Leary, J.K., Micheli, F., Airoldi, L., Boch, C., De Leo, G., Elahi, R., Ferretti, F., Graham, N.A.J., Litvin,
941   S.Y., Low, N.H., Lummis, S., Nickols, K.J., Wong, J., 2017. The Resilience of Marine Ecosystems
942   to Climatic Disturbances. BioScience 67, 208–220. https://doi.org/10.1093/biosci/biw161

943   Olivier, J.-M., Dole-Olivier, M.-J., Amoros, C., Carrel, G., Malard, F., Lamouroux, N., Bravard, J.-P., 2009.

944   Chapter 7 - The Rhône River Basin, in: Tockner, K., Uehlinger, U., Robinson, C.T. (Eds.), Rivers

945   of Europe. Academic Press, London, pp. 247–295. https://doi.org/10.1016/B978-0-12-369449-

946   2.00007-2

947   Palacín, C., Gili, J.-M., Martín, D., 1992. Evidence for coincidence of meiofauna spatial heterogeneity

948   with eutrophication processes in a shallow-water Mediterranean bay. Estuarine, Coastal and

949   Shelf Science 35, 1–16. https://doi.org/10.1016/S0272-7714(05)80053-8

950   Palmer, M.A., Gusf, G., 1985. Dispersal of meiofauna in a turbulent tidal creek. Journal of Marine

951   Research 43, 179–210. https://doi.org/10.1357/002224085788437280

952   Palmer, M.A., Montagna, P.A., Spies, R.B., Hardin, D., 1988. Meiofauna dispersal near natural

953   petroleum seeps in the Santa Barbara channel: A recolonization experiment. Oil and Chemical

954   Pollution 4, 179–189.

955   Pastor, L., Deflandre, B., Viollier, E., Cathalot, C., Metzger, E., Rabouille, C., Escoubeyrou, K., Lloret, E.,

956   Pruski, A.M., Vétion, G., Desmalades, M., Buscail, R., Grémare, A., 2011a. Influence of the

957   organic matter composition on benthic oxygen demand in the Rhône River prodelta (NW

958   Mediterranean Sea). Continental Shelf Research 31, 1008–1019.

959   https://doi.org/10.1016/j.csr.2011.03.007

960   Pastor, L., Rabouille, C., Metzger, E., Thibault de Chanvalon, A., Viollier, E., Deflandre, B., 2018.

961   Transient early diagenetic processes in Rhône prodelta sediments revealed in contrasting

962   flood events. Continental Shelf Research 166, 65–76.

963   https://doi.org/10.1016/j.csr.2018.07.005

964   Payrastre, O., Naulin, J.P., Nguyen, C.C., Gaume, E., 2012. Analyse hydrologique des crues de juin 2010

965   dans le Var (Rapport de recherche). IFSTTAR - Institut Français des Sciences et Technologies

966   des Transports, de l'Aménagement et des Réseaux.

967   Pelletier, É., Deflandre, B., Nozais, C., Tita, G., Desrosiers, G., Gagné, J.-P., Mucci, A., 1999. Crue éclair

968   de juillet 1996 dans la région du Saguenay (Québec). 2. Impacts sur les sédiments et le biote

969   de la baie des Ha! Ha! et du fjord du Saguenay. Canadian Journal of Fisheries and Aquatic

970   Sciences. 56, 2136–2147. https://doi.org/10.1139/f99-143

971   Pont, D., Simonnet, J.-P., Walter, A.V., 2002. Medium-term Changes in Suspended Sediment Delivery

972   to the Ocean: Consequences of Catchment Heterogeneity and River Management (Rhône

973   River, France). Estuarine, Coastal and Shelf Science 54, 1–18.

974   https://doi.org/10.1006/ecss.2001.0829

975   Pruski, A.M., Buscail, R., Bourgeois, S., Vétion, G., Coston-Guarini, J., Rabouille, C., 2015.

976   Biogeochemistry of fatty acids in a river-dominated Mediterranean ecosystem (Rhône River

977   prodelta, Gulf of Lions, France): Origins and diagenesis. Organic Geochemistry 83–84, 227–

978   240. https://doi.org/10.1016/j.orggeochem.2015.04.002

979   Rabouille, C., 2010a. MESURHOBENT 1 cruise,Téthys II R/V. https://doi.org/10.17600/10450020

980   Rabouille, C., 2010b. MESURHOBENT 2 cruise,Téthys II R/V. https://doi.org/10.17600/10450060

981   Rabouille, C., 2010c. MESURHOBENT 3 cruise,Téthys II R/V. https://doi.org/10.17600/10450100

982   Rabouille, C., 2010d. MESURHOBENT 4 cruise,Téthys II R/V. https://doi.org/10.17600/10450140

983   Rabouille, C., Denis, L., Dedieu, K., Stora, G., Lansard, B., Grenz, C., 2003. Oxygen demand in coastal

984   marine sediments: comparing in situ microelectrodes and laboratory core incubations. Journal

985   of Experimental Marine Biology and Ecology 285–286, 49–69. https://doi.org/10.1016/S0022-

986   0981(02)00519-1

987   Rassmann, J., Eitel, E.M., Lansard, B., Cathalot, C., Brandily, C., Taillefert, M., Rabouille, C., 2020.

988   Benthic alkalinity and dissolved inorganic carbon fluxes in the Rhone River prodelta generated

989   by decoupled aerobic and anaerobic processes. Biogeosciences 17, 13–33.

990   https://doi.org/10.5194/bg-17-13-2020

991   Riera, P., Hubas, C., 2003. Trophic ecology of nematodes from various microhabitats of the Roscoff

992   Aber Bay (France): importance of stranded macroalgae evidenced through $\delta13C$ and $\delta15N$.

993   Marine Ecology Progress Series 260, 151–159. https://doi.org/10.3354/meps260151

994   Rudnick, D., 1989. Time lags between the deposition and meiobenthic assimilation of phytodetritus.

995   Marine Ecology Progress Series 50, 231-240. https://doi.org/10.3354/meps050231

996   Salen-Picard, C., Arlhac, D., Alliot, E., 2003. Responses of a Mediterranean soft bottom community to

997   short-term (1993-1996) hydrological changes in the Rhône river. Marine Environmental

998   Research 55, 409–427.

999   Schratzberger, M., Ingels, J., 2018. Meiofauna matters: The roles of meiofauna in benthic ecosystems.

1000   Biology and Ecology 502, 125-25.

1001   Schratzberger, M., Whomersley, P., Warr, K., Bolam, S.G., Rees, H.L., 2004. Colonisation of various

1002   types of sediment by estuarine nematodes via lateral infaunal migration: a laboratory study.

1003   Marine Biology 145, 69–78. https://doi.org/10.1007/s00227-004-1302-1

1004   Scott, D.B., Tobin, R., Williamson, M., Medioli, F.S., Latimer, J.S., Boothman, W.A., Asioli, A., Haury, V.,

1005   2005. Pollution monitoring in two North American estuaries: historical reconstructions using

1006   benthic   foraminifera.   Journal   of   Foraminiferal   Research   35,   65–82.

1007   https://doi.org/10.2113/35.1.65

1008   Semprucci, F., Balsamo, M., Appolloni, L., Sandulli, R., 2018. Assessment of ecological quality status

1009   along the Apulian coasts (eastern Mediterranean Sea) based on meiobenthic and nematode

1010   assemblages. Mar Biodiv 48, 105–115. https://doi.org/10.1007/s12526-017-0745-9

1011   Semprucci, F., Facca, C., Ferrigno, F., Balsamo, M., Sfriso, A., Sandulli, R., 2019. Biotic and abiotic

1012   factors affecting seasonal and spatial distribution of meiofauna and macrophytobenthos in

1013   transitional   coastal   waters.   Estuarine,   Coastal   and   Shelf   Science,   219,   328–340.

1014   https://doi.org/10.1016/j.ecss.2019.02.008

1015   Shimanaga, M., Kitazato, H., Shirayama, Y., 2000. Seasonal Patterns of Vertical Distribution between

1016   Meiofaunal Groups in Relation to Phytodetritus Deposition in the Bathyal Sagami Bay, Central

1017   Japan. Journal of Oceanography 56, 379–387. https://doi.org/10.1023/A:1011120204419

1018   Soetaert, K., Vincx, M., Wittoeck, J., Tulkens, M., 1995. Meiobenthic distribution and nematode

1019   community structure in five European estuaries. Hydrobiologia 311, 185–206.

1020   https://doi.org/10.1007/BF00008580

1021   ter Braak, C.J.F., 1986. Canonical Correspondence Analysis: A New Eigenvector Technique for

1022   Multivariate   Direct   Gradient   Analysis.   Ecology   67,   1167–1179.

1023   https://doi.org/10.2307/1938672

1024   Tesi, T., Langone, L., Goñi, M.A., Miserocchi, S., Bertasi, F., 2008. Changes in the composition of

1025   organic matter from prodeltaic sediments after a large flood event (Po River, Italy).

1026   Geochimica et Cosmochimica Acta 72, 2100–2114. https://doi.org/10.1016/j.gca.2008.02.005

1027   Ulses, C., Estournel, C., Durrieu de Madron, X., Palanques, A., 2008. Suspended sediment transport in

1028   the Gulf of Lions (NW Mediterranean): Impact of extreme storms and floods. Continental Shelf

1029   Research 28, 2048–2070. https://doi.org/10.1016/j.csr.2008.01.015

1030   Vanaverbeke, J., Steyaert, M., Soetaert, K., Rousseau, V., Van Gansbeke, D., Parent, J.-Y., Vincx, M.,

1031   2004. Changes in structural and functional diversity of nematode communities during a spring

1032   phytoplankton bloom in the southern North Sea. Journal of Sea Research 52, 281–292.

1033   https://doi.org/10.1016/j.seares.2004.02.004

1034   Vanreusel, A., Vincx, M., Schram, D., Gansbeke, D. van, 1995. On the Vertical Distribution of the

1035   Metazoan Meiofauna in Shelf Break and Upper Slope Habitats of the NE Atlantic.

1036   Internationale Revue der gesamten Hydrobiologie und Hydrographie 80, 313–326.

1037   https://doi.org/10.1002/iroh.19950800218

1038   Villora-Moreno, S., 1997. Environmental Heterogeneity and the Biodiversity of Interstitial Polychaeta.

1039   Bulletin of Marine Science 60, 494–501.

1040

1041   Table 1: Principal descriptors used in this study with their interpretation.

Descriptors	Feature	Main diagnostic information	References
C/N	Source/Quality	Marine derived OM (6-9), Soil derived OM (8-20) and higher plants (>20); may decrease during OM decomposition	Moloney and Field (1991), Hedges and Oades (1997), Meyers (1997)
δ^{13}C	Source	Marine OM (–20.1±0.8‰) and Rhône River inputs (–27.1 ± 0.6‰)	Harmelin-Vivien et al. (2008) and Higueras et al. (2014)
DI	Quality	Diagenetic alteration of OM with DI values ranging from –2.2 extensively degraded sediments to -1.5 for fresh algae	Dauwe et al. (1999b)
RI	Quality	Selective degradation during diagenesis and production of non-proteic amino acids, lower values in degraded sediments	Jennerjahn & Ittekkot (1997)
EHAA/THAA (%)	Quality	OM bioavailability for the benthic fauna ranging from 0 to 100%	Mayer et al. (1995)
MC-SAFA	Source	Mixed origin, but shorter chains predominate in phytoplankton	Dunstan et al. (1994), Bianchi and Canuel (2011)
LC-SAFA	Source	Terrestrial higher plants, macrodetritus	Bianchi and Canuel (2011), Dunstan et al. (1994), Pruski et al. (2015)
Ter PUFA	Source	Terrestrial higher plants (>2.5%)	Budge et al. (2001), Pruski et al. (2015)
Algal PUFA	Source	Phytoplankton with $C_{20:5\omega3}$ specific of diatoms	Dunstan et al. (1994)
MUFA	Source	Mixed origin with $C_{16:1\omega7}$ common in diatoms and bacteria	Bianchi and Canuel (2011), Dunstan et al. (1994)
BAFA	Source	Bacterial sources	Bianchi and Canuel (2011)

1042   The degradation index (DI), reactivity index (RI) and enzymatically hydrolysable amino acids to total hydrolysable amino acids ratio (EHAA/THAA) are
1043   inferred from the amino acid composition. Fatty acid biomarkers are grouped as follows: mid-chain even-number saturated fatty acids with less than 20
1044   carbons (MC-SAFAs), long-chain saturated fatty acids with 24 carbon or more (LC-SAFA), polyunsaturated fatty acids with 18 carbons ($C_{18:2\omega6}$ and $C_{18:3\omega3}$,
1045   Terr PUFA), the remaining PUFA attributed to microalgae (Algal PUFA), the monounsaturated fatty acids (MUFA) and the straight and branched odd-
1046   numbered fatty acids of bacterial origin (BAFA). The unsaturation index is calculated as the sum of products of the number of double bonds of each acid
1047   multiplied by its percentage of the total fatty acid composition.

1048

1049   Table 2: Temporal variations of Diffusive Oxygen Uptake (DOU) rates in the sediments of the Rhône

1050   **River prodelta in April, July and August 2010.** Values are means ± standard deviations (n= 4), nd= not

1051   determined.

1052

Stations	DOU		
	April 2010	**July 2010**	**August 2010**
MESURHO	16.9 ± 4.1	10.1 ± 0.6	9 ± 1.5
A	14.9 ± 1.3	10.6 ± 3.6	nd
AK	19.7 ± 3.5	11.4 ± 1.3	nd
B	12.7 ± 2.1	11.3 ± 2.9	nd
K	14.9 ± 2.6	11.8 ± 4.9	nd

1053

1054

1055 **Table 3:** Marginal and conditional effects of environmental variables determined using forward selection. Ranking is based on their P-value and Akaike
1056 Information Criterion (AIC) where the variable with the lowest AIC value is the most influential. 999 permutations. Significant variables are indicated in
1057 bold, * p<0.05, ** p<0.01. Best combination of variables: Porosity + δ^{13}C + DI.

1058

1059

Marginal effects						Conditional effects					
Rank	Variable	AIC	F ratio	Pr(>F)		Rank	Variable	AIC	F ratio	Pr(>F)	
1	**Porosity**	79.935	7.267	0.005	**	1	**Porosity**	79.935	7.267	0.005	**
2	**Algal PUFA**	81.865	5.0518	0.005	**	2	**δ^{13}C**	78.509	3.2544	0.015	*
3	**EHAA**	81.042	5.9774	0.015	**	3	**DI**	77.785	2.4517	0.045	*
4	C/N	85.621	1.1536	0.270		-	EHAA	78.170	1.3657	0.180	
5	δ^{13}C	85.715	1.0625	0.385		-	Clay	78.285	1.2658	0.290	
6	EHAA/THAA	86.120	0.6742	0.575		-	Algal PUFA	78.507	1.0746	0.400	
7	DI	86.174	0.6229	0.605		-	EHAA/THAA	79.305	0.3983	0.795	
8	$CaCO_3$	86.252	0.5482	0.655		-	$CaCO_3$	79.301	0.4013	0.820	
9	Clay	86.343	0.4626	0.715		-	C/N	79.419	0.303	0.925	

1060

Highlights:

- Vertical distribution of sedimentary organics varies at a monthly time scale

- Origin determines organic matter quality

- Meiofaunal abundances are driven by trophic conditions and river regime

- Rapid response of meiofauna to the sedimentation of phytodetritus

- High resilience of meiofauna to flood disturbance

Highlights:

Declaration of interests

☒ The authors declare that they have no known competing financial interests or personal relationships that could have appeared to influence the work reported in this paper.

☒The authors declare the following financial interests/personal relationships which may be considered as potential competing interests:

Dr Audrey Pruski, on behalf of all co-authors